# CONTRAST ENHANCEMENT BY LATERAL INHIBITION IN A SENSORY NETWORK

**A Thesis submitted to**
**the Graduate School of Engineering and Science of**
**Izmir Institute of Technology**
**in Partial Fulfillment of the Requirements for the Degree of**

**MASTER OF SCIENCE**

**in Materials Science and Engineering**

**by**
**Anıl COŞKUN**

**July 2006**
**Izmir, Turkey**

We approve the thesis of **Anıl COŞKUN**

**Date of Signature**

..... **14 July 2006**
**Asst. Prof. Dr. Serhan ÖZDEMİR**
Supervisor
Department of Mechanical Engineering
Izmir Institute of Technology

..... **14 July 2006**
**Assoc. Prof. Dr. Metin TANOĞLU**
Co-Supervisor
Department of Mechanical Engineering
Izmir Institute of Technology

..... **14 July 2006**
**Asst. Prof. Dr. Şevket GÜMÜŞTEKİN**
Department of Electrical and Electronics Engineering
Izmir Institute of Technology

..... **14 July 2006**
**Asst. Prof. Dr. Gürsoy TURAN**
Department of Civil Engineering
Izmir Institute of Technology

..... **14 July 2006**
**Assoc. Prof. Dr. Mustafa GÜDEN**
Department of Mechanical Engineering
Izmir Institute of Technology

..... **14 July 2006**
**Prof. Dr. Muhsin ÇİFTÇİOĞLU**
Head of Department
Izmir Institute of Technology

……
**Assoc. Prof. Dr. Semahat Özdemir**
Head of the Graduate School

# ACKNOWLEDGEMENTS

I would like to express my gratitude to my advisor Asst. Prof. Dr. Serhan Özdemir and my co-advisor Assoc. Prof. Dr. Metin Tanoğlu for their invaluable advice, guidance, and encouragement. I would like to thank the IYTElligence laboratory staff for their help during my study.

I would also like to thank my friends Elçin Dilek Kaya, Emrah Bozkurt and Kıvanç Işık for their encouragement, help and patience.

I am also grateful to my parents for their endless support during my thesis and all of my life.

# ABSTRACT

## CONTRAST ENHANCEMENT BY LATERAL INHIBITION IN A SENSORY NETWORK

The most important mechanism to occur in biological distributed sensory networks (DSNs) is called "Lateral Inhibition, (L.I.)". L.I. relies on one simple principle. Each sensor strives to suppress its neighbors in proportion to its own excitation. L.I. is found all around the human nervous and sensory system. In audition, for example lateral inhibition occurs at the relay points on the way up to the brain. It is realized that L.I. must not be limited to biosystems. Any artificial system claiming to have a discriminating tactile sensing, say like a robotic hand, ought to carry a redundancy reduction and contrast enhancement tool similar to L.I.

In this study, lateral inhibition mechanism was analyzed and simulated. To simulate the LI. mechanism an experimental set-up was built up. The effects of LI. mechanism were observed in an artificial sensory network that contained photodiodes. The sensors in the networks were stimulated by a halogen light source that can be moved in three axes. The results showed that LI. is not only functional for biological DSNs but also for artificial DSNs.

LI. mechanism was also used to localize an unknown position of light source that illuminated the photosensitive sensory network containing high and low quality sensors. Each photosensitive sensor was calibrated relative to the distance to the light source. The output of each sensor was converted into a distance reading according to the calibration and this was employed to localize the position of the light source. Results showed that lateral inhibition mechanism increased the sensitivity of localization and it gave an ability to low quality sensors to make localization as sensitive as high quality sensors.

# ÖZET


BİR SENSÖR AĞINDA LATERAL İNHİBİSYON YOLU İLE KONTRAST ARTTIRIMI

Biyolojik sensör ağlarında gözlenen en önemli mekanizma 'Lateral İnhibisyon (L.İ.)' olarak adlandırılır. L.İ. oldukça basit bir prensip üzerinde temellendirilmiştir. Her bir sensör komşu olduğu sensörleri kendi gücü oranında bastırmaya çalışır. Lateral inhibisyon mekanizması insan sinir sisteminde ve sensör sisteminde de bulunmaktadır. Örneğin işitme sisteminde, kulaktan beyine giden sinir sisteminin çeşitli iletim noktalarında lateral inhibisyon oluşur. L.İ. mekanizması sadece biyolojik sistemler için geçerli değildir. Herhangi bir yapay sensör sisteminde de L.İ. mekanizmasının sonuçlarından olan kontrast arttırımı ya da gereksiz bilginin azaltılması gibi etkiler görülür.

Bu çalışmada lateral inhibisyon mekanizması incelendi. Lİ. mekanizmasının etkilerini görebilmek için bir deney düzeneği oluşturuldu. Fotodiyotlardan oluşturulmuş sensör grupları üzerinde Lİ. mekanizmasının etkileri gözlemlendi. Kullanılan sensör grupları, üç eksende hareket edebilen bir halojen ışık kaynağı kullanılarak tahrik edildi. Sonuçlar gösterdi ki, Lİ. sadece biyolojik sensör grupları için değil aynı zamanda yapay sensör grupları için de işlevsel bir mekanizmadır.

Bu çalışma kapsamında Lİ. mekanizması, koordinatları bilinmeyen bir ışık kaynağı tarafından aydınlatılan, yüksek kaliteli ya da düşük kaliteli ışığa duyarlı sensor grupları üzerine uygulanarak, ışık kaynağının pozisyonunun tespitinde kullanıldı. Her bir sensor ışık kaynağı ile arasındaki mesafeye bağlı olarak kalibre edildi. Kalibrasyon kullanılarak her bir sensörden okunan değerler mesafe bilgisine çevrildi ve bu ışık kaynağının yerinin tespitinde kullanıldı. Deneyler sonucunda Lİ. mekanizmasının kullanımının, pozisyon tespitindeki hatayı azalttığı ve düşük kaliteli sensörler ile yapılan yer tespitinin yüksek kaliteli olanlarla yapılanlar kadar hassas sonuçlar vermesini sağladığı gözlemlendi.

# TABLE OF CONTENTS

# LIST OF FIGURES

# LIST OF TABLES

# CHAPTER 1

# INTRODUCTION

Detection and monitoring requires that at least one sensor or an array of sensors be employed. Some applications necessitate that the detailed analysis of natural phenomena must be accomplished by two or more sensors that are distributed to observation area. A set of geographically scattered sensors designed to collect information about the environment in which they are deployed are described as a *distributed sensory network* (DSN). Today many advanced systems employ distributed sensory systems which consist of a large number of sensors in practical applications ranging from aerospace and defence, robotics and automation systems, to monitoring and control of process generation plants. However distributed sensory networks (DSNs) have a large application areas, the development and implementation of DSN systems bring about a combination of many different problems in sensor deployment such as network communication, data association, fusion and processing. Although long processing time and excessive consumed energy for processing of information are common problems for DSNs, the primary reason of all these problems that described above and the most important challenge to overcome for DSNs is redundancy. Depending on the increasing number of sensors used in DSN, the input fields of the individual sensors may overlap, leading to redundancy. Although there are many techniques in order to cope with the redundancy problem, *lateral inhibition* (LI) stands out for its ubiquity and simplicity.

LI is a basic peripheral processing principle in biological systems such as visual, auditory and somatosensory systems. It is commonplace in biological distributed sensory networks. In lateral inhibition mechanism, each individual receptor drives down each of its neighbours in proportion to its own excitation.

While the first attempts to describe lateral inhibition were made by Ernst Mach on the basis of his perceptual experiments demonstrating Mach bands, H.K.Hartline constituted the first statement based on known interactions of biological sensors. The concept of lateral inhibition arose in the extensive experimental research of Hartline and his colleagues on the facetted compound eye of Horseshoe crab (Limulus). This

research occupied a period of over fifty years and is an outstanding example of bringing quantitative mathematical methods of signal transmission to bear on a biological preparation.

Barlow, was a student of Hartline who continued to explore vision in Horseshoe crab and who studied how lateral inhibition influenced behaviour. He found that male horseshoe crabs were able to distinguish shapes and shades of colour. He placed concrete casts of adult female crabs, a hemispherical cast and a cube both of which approximated the size of a female crab. He also painted these casts either black, grey, or white. He found that the crabs were attracted to the castings and that they showed preference to the black crab-shape and the white cube received the least attention.

Brooks discussed the features of biological sensors and possible ramifications that might occur, should there be a parameter change. The dominant feature of distributed sensory networks is lateral inhibition, where each sensor drives down each of its neighbours in proportion to its own excitation.

Seung et al. showed that there is a competition between neurons thanks to lateral inhibition. This is popularly known as winner-take-all competition. They set a formula to show the inhibitory connectivity of overlapping groups. Their study stated that it was possible to organize lateral inhibition to mediate the winner-take-all competition between potentially overlapping groups of neurons.

This thesis presents the principles and effects of the lateral inhibition mechanism. The role of lateral inhibition in human sensory and nervous system was analysed. Advantages of lateral inhibition in human auditory, visual and somatosensory systems were portrayed. Its effects such as contrast enhancement, funnelling and two point discrimination were examined and these effects were observed on an experimental setup which contained photosensitive sensors.

The influences of lateral inhibition mechanism on the distributed sensory network were examined by constructing an experimental setup which contained distributed photosensitive sensory network. The unknown position of stimulant such as light source was localized by employing sensory network with and without applying lateral inhibition mechanism.

The aim of this study is to show the effect of lateral inhibition mechanism on target localization. For this purpose, several sensory arrays which contain *light dependent resistors* or *photodiodes* with different configurations had been constructed and the unknown position of a light source (target) was estimated by measuring the

outputs of these sensory arrays. As a first step, the single member of each sensor group (LDRs and photodiodes) was illuminated by adjusting the light source to different positions whose coordinates were known and the response of sensors were recorded. This process could aptly be called calibration. Then the light source was placed on an unknown position on the sensory array and depending on the calibration the distances between sensors and the light source were estimated. Then the lateral inhibition mechanism was applied to the sensor outputs and this process modified the response of the sensors. These estimated and modified values were used to find the position of the light source by applying a method known as *trilateration* and a $TbhP^{+}$ - given in appendix A - algorithm written in the Matlab© programming language.

# CHAPTER 2

# LATERAL INHIBITION

## 2.1. What Is Lateral Inhibition

Lateral inhibition (L.I.) is the dominant feature of distributed sensory networks where each individual receptor drives down each of its neighbours in proportion to its own excitation. The strengths of these connections are fixed rather than modifiable and are generally arranged as excitatory among nearby receptors and inhibitory among farther receptors. In other words, when any given receptor responds, the excitatory connections tend to increase its response while inhibitory connections try to decrease it . All receptors in the network receive a mixture of excitatory and inhibitory signals from other competitive receptors. As a result of the competitive network structure a distinction between the receptor or a group of receptors which have the strongest output and the receptors with weaker output become larger. Weaker receptors might be suppressed. According to the value of excitatory and inhibitory coefficients and number of interconnected receptors, the response of the whole network can vary. In the case of choosing optimum coefficients, the receptor which has the strongest output suppresses all the other receptor outputs and this kind of a network is called "winner take all" type.

Lateral inhibition is a basic peripheral processing phenomenon for biological systems. It is commonplace in human nervous system and it has been widely recognized as contrast enhancement mechanism by biologists (Brooks 1988). It is also sometimes called on-center or off-surround architecture. These terms are especially used for biological structures that operate in the same way.

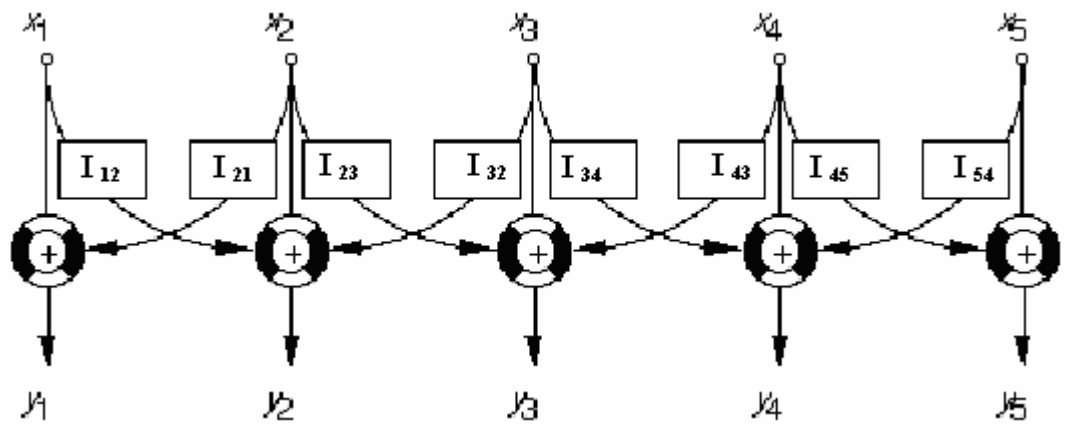


Figure 2.1 Schematic illustration of Lateral Inhibition

Figure 2.1 defines a set of sensors with lateral inhibition mechanism. The arcs ending in black arrows indicate inhibitory effect of each sensor on the neighbours sensors which are represented by "I". Each individual sensor has individual input that is designated by "$x_n$" and each sensor drives down the output "$y_n$" of its neighbours which are connected to it at black arrow end. The ratio between the amount of sensory output which is driven down by neighbours and the amount of output is called the degree of lateral inhibition.

## 2.2. Historical Background Of Lateral Inhibition

Effects of lateral inhibition were first recognized in 1886 by the Austrian physicist Ernst Mach who ascertained that all knowledge was based on sensation, and that all scientific observations or measurements were dependent upon the observer's perception. Although the physiological phenomenon discovered by him was not named lateral inhibition, it was the first step for future studies. Mach's study concluded that the brighter and darker contours are physiologically provoked. There is a brightness enhancement at the region where the bright area becomes darker and there is a darker band where the dark area becomes brighter. This effect can be seen in Figure 2.2.

Figure 2.2 Illustration of Mach Band.

Although there are two columns which have different but constant physical brightness values near the border line of the two columns, a dissimilarity is perceived by observers. It is seen that dark column becomes brighter and bright column becomes darker near the border line.

The most important studies that explained the lateral inhibition mechanism were made by H.K. Hartline in 1934, who received Nobel prize for this work in 1968. His works were about visual system of Horseshoe crab (Limulus polyphemus) which is a kind of arthropod from North America (Figure 2.3). The concept of lateral inhibition arose in the comprehensive experimental research of H.K.Hartline and colleagues on the facetted compound eye of Horseshoe crab. This research proceeded a period of over fifty years and was an outstanding example of bringing quantitative mathematical methods of signal transmission.

### 2.2.1. Horseshoe Crab (Limulus polyphemus)

Horseshoe crabs (Figure 2.3) are among the world's oldest and most impressive creatures. They are estimated to be at least 300-million years old. The horseshoe crab belongs to the large group of invertebrates (animals without backbones) called Arthropods. The earliest horseshoe crab species were crawling around the Earth's shallow coastal seas for at least 100-million years before even the dinosaurs arrived. Since that time, the Earth's land masses have shifted dramatically, thousands of other species have come and gone, but horseshoe crabs have survived and today remain much

as they were those millions of years ago. Horseshoe crabs have been used by people for centuries. More recently, they have been instrumental to scientific research especially in biomedical fields.

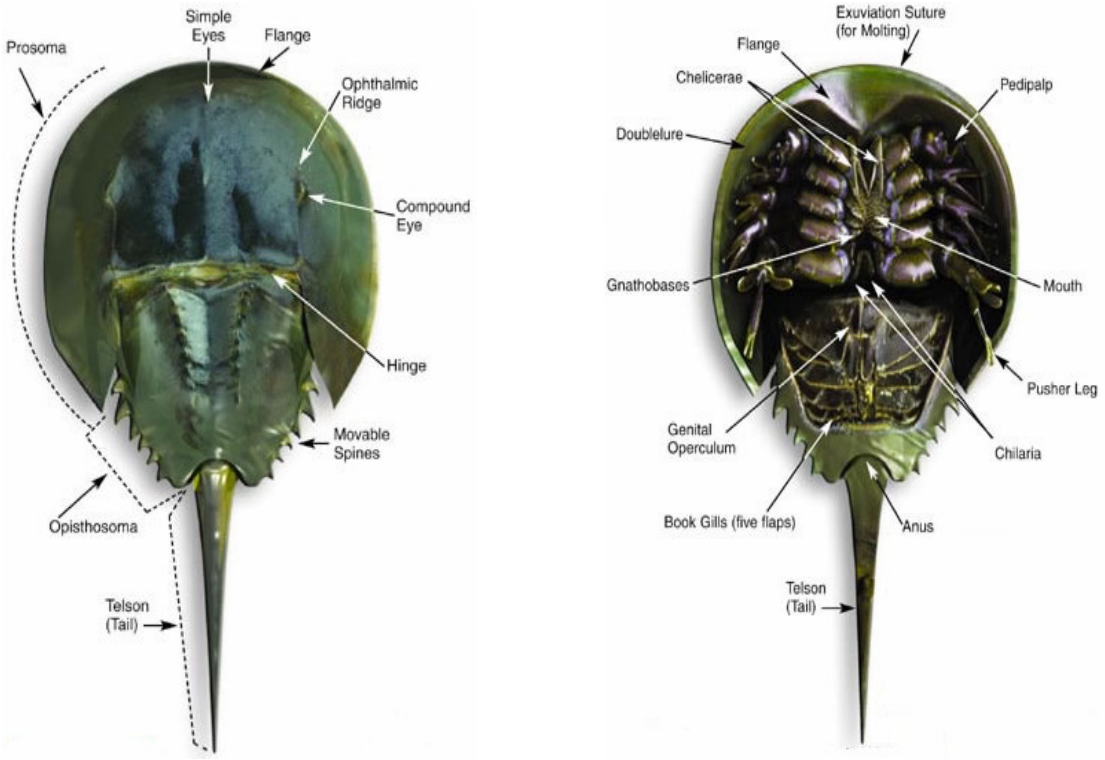


Figure 2.3 Dorsal and ventral view of Horseshoe Crab
(Source: WEB_1 2005)

The horseshoe crab is the most well-studied invertebrate in the world, and several Nobel Prizes have been awarded to researchers based on their work on horseshoe crabs. Researchers have discovered that chitin, which makes up the horseshoe crab's shell, can shorten the healing time of wounds by 35- 50% and reduces pain compared to other standard treatment. Chitin is now used to make dressings and sutures for burns, surface wounds, and skin-graft donor sites. About 30 years ago, scientists discovered that horseshoe crab blood clots in the presence of small amounts of bacterial toxins. The chemical in their blood responsible for this clotting is called Limulus Amoebocyte Lysate (LAL). Currently, LAL is in high demand worldwide as the most effective substance used to test for bacterial contamination in commercial drugs and medical equipment. During the past 50 years, research on the compound eyes of horseshoe crabs has lead to a better understanding of how human eyes function. Basic

reasons of using Horseshoe crab for scientific studies especially about vision studies are:

- For a marine animal Horseshoe crab is also quite hardy.
- Horseshoe crab can be safely kept out of water for relatively long periods of time.
- The compound eyes of Horseshoe crab are relatively large.
- Horseshoe crab optic nerve, which connects the eyes to the brain is not very long.

### 2.2.2. Horseshoe Crab Vision And Lateral Inhibition

Horseshoe crabs have a total of ten eyes used for finding mates and feeding by sensing light. The most obvious eyes are the two lateral eyes which are used for finding mates during the spawning season. These eyes are also called compound eyes. The compound eyes are made of smaller, simple eye units, called ommatidia (Figure 2.4). Each compound eye has about 1,000 receptors or ommatidia. The cones and rods of the lateral eyes have similar structure to those found in human eyes. Except that they are around 100 times larger in size (Figure 2.5).

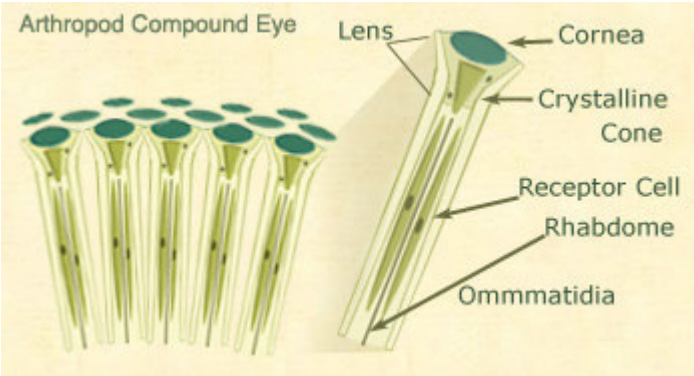


Figure 2.4. Illustration of compound eye consist of ommatidia
(Source: WEB_1 2005)

As shown schematically in Figure 2.6(a), the cylindrical corneal lens which is represented by ”l” of each ommatidium focuses incident light through an aperture which

is represented by “a” formed by the processes of pigment cells represented by “p” onto the photosensitive rhabdomeres indicated by “b” of 10–12 retinular cells marked by “r”.

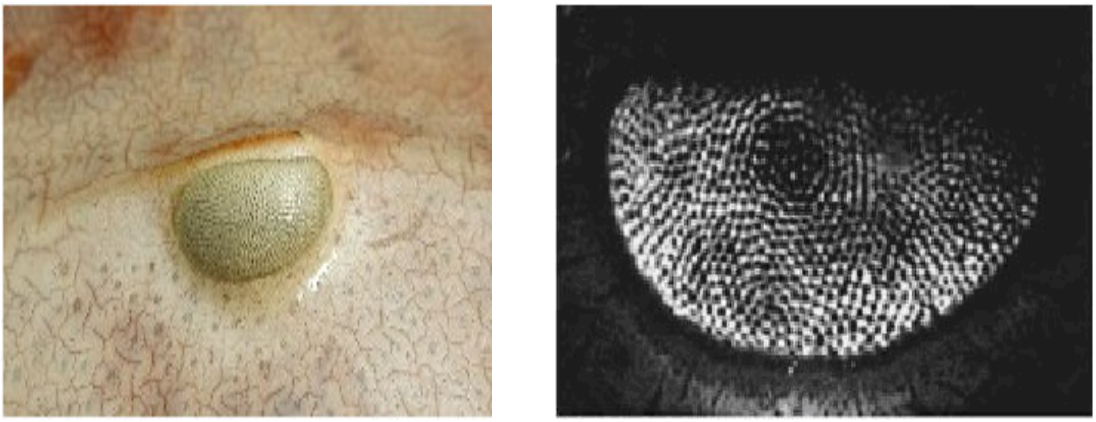

(a) (b)

Figure 2.5. Compound eye of Horseshoe Crab. (a) Real photo of compound eye (b) Close up view of compound eye of Horseshoe Crab (Source : Passaglia et al. 1998)

Each retinular cell transduces the incident light into a photocurrent that flows passively into the eccentric cell which is represented by “e” through gap junctions in its dendrite. The individual photocurrents of retinular cells sum together in the eccentric cell forming a depolarizing ‘‘receptor potential’’ that is readily recorded with a microelectrode impaling the soma of the eccentric cell. The summed excitatory photocurrent propagates passively through the soma and down the axon to the spike-generation site which is marked by “x”. Self- and lateral-inhibitory currents which take place in part “i” triggered by the spikes of the eccentric cell itself and those of its neighbours also propagate to the spike-generation site via a dense neuropil of synaptic connections.

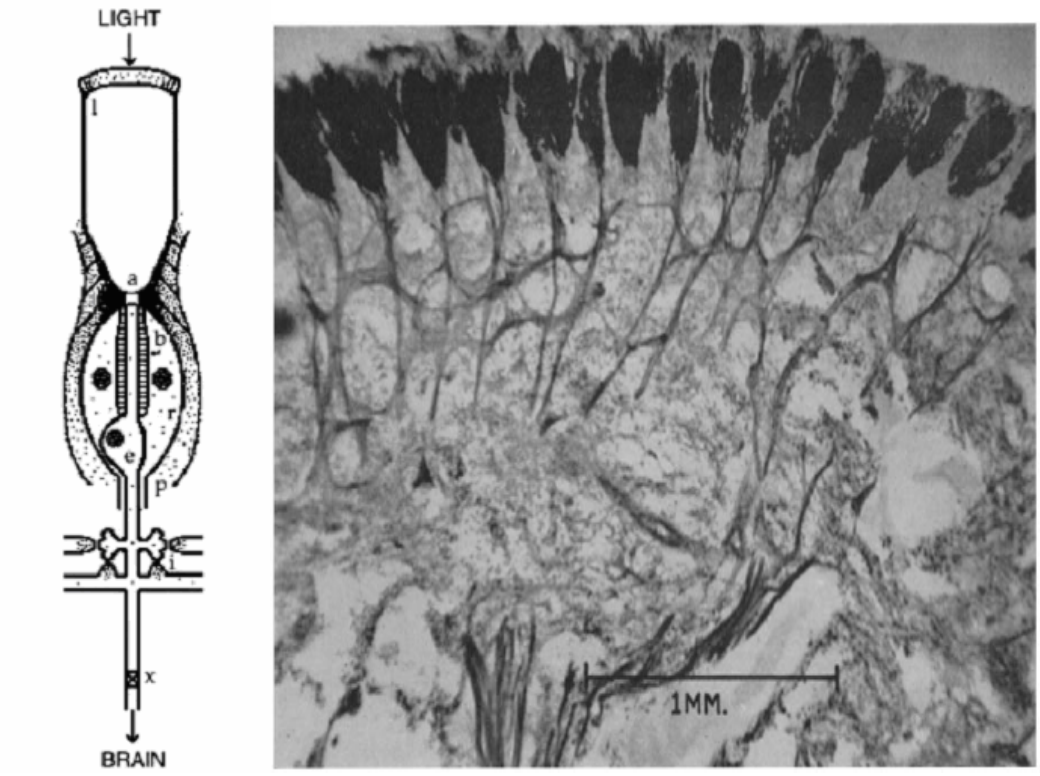


(a) (b)

Figure 2.6. (a) Structure of single ommaditium. (b) Section through part of a lateral eye of an adult Horseshoe Crab, showing a cluster of ommatidia (Source : Hartline et.al 1955 , Passaglia et al. 1998)

There the excitatory and inhibitory currents sum to produce a ‘‘generator potential’’ that the spike generator encodes as a train of action potentials. The spike train propagates backward to the soma and along axon collaterals to exert self- and lateral inhibition and forward along the optic nerve to the brain to mediate behaviour. The block diagram of Figure 2.7 outlines how optical and neural mechanisms of an ommatidium combine in the Horseshoe Crab eye.

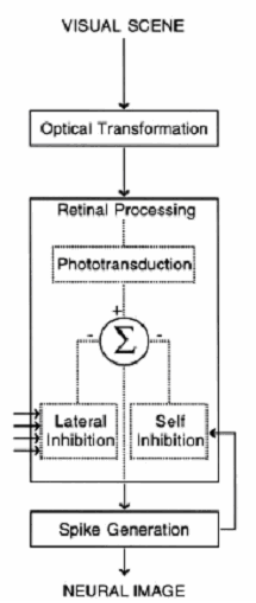


Figure 2.7. Schematic demonstration of optical and neural mechanism of ommaditium. (Source: Passaglia et al. 1998)

The earlier experiment which have done with Horseshoe Crab proved that the main visual requirement for Horseshoe Crab vision is contrast and lateral inhibition mechanism enhances ability of Horseshoe Crab to distinguish contrast. This phenomenon can be seen in Figure 2.8 and it will be discussed in the following chapter.

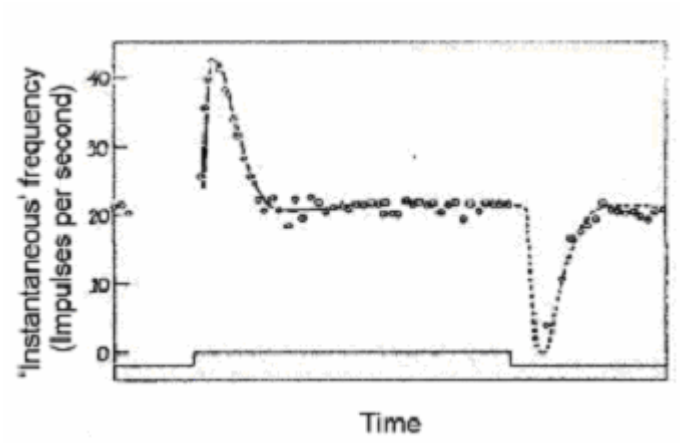


Figure 2.8. Effect of Lateral Inhibition on distinguishing contrast ( Source: Ratliff et al. 1963)

During the day, horseshoe crabs are attracted to colours most similar to the colour of a normal horseshoe crab carapace, during the night, white targets are actually attracted more than grey, presumably because, in the reduced illumination, the horseshoe crab was unable to discriminate the grey target from the sandy bottom, and the white target apparently provided enough contrast in the darkness to be discriminated (Barlow et al. 1982). However, in all circumstances, a dark object on light background attracted the most. As shown in Figure 2.9 during the day, the resolution of a neural image of visual stimulus is better than the night resolution of neural image of almost the same visual stimulus.

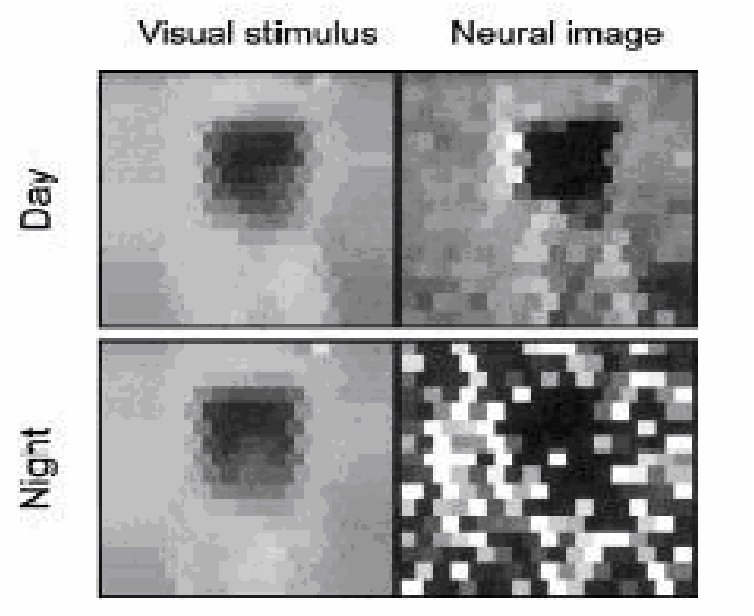


Figure 2.9. Resolution that Horseshoe Crab can achieve with respect to the light (Source: Barlow et al. 2001)

## 2.3. Mathematical Formulation Of Lateral Inhibition

As mentioned in earlier sections, the mechanism of lateral inhibition is defined as a result of experiments which were carried out on the visual system of Horseshoe Crab. All studies are based on the measurement of the frequency of the discharge of nerve impulses from receptor units which are stimulated by light source. The responses (impulses) of each receptor unit (ommatidium) were recorded by an oscillogram.

At the beginning, two small strands were dissected from the optic nerve and connected to the impulse recording system. Then a small spot of light was projected on the strand. To observe the mutual interaction between the two strands (receptor unit) they were illuminated together and separately. Oscillograms of the frequency of nerve fiber (strand) impulses were recorded photographically in some experiment (Figure 2.10).

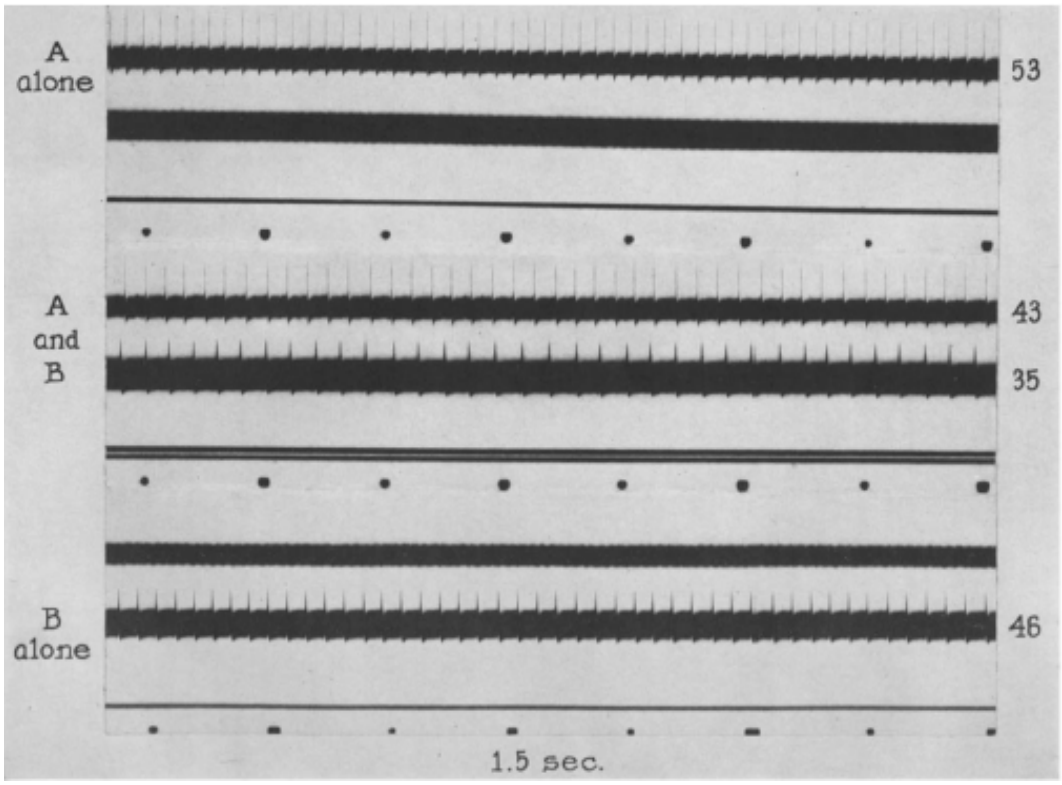


Figure 2.10. Oscillograms of nerve fiber (strand) impulse frequency of the lateral eye of Horseshoe Crab. (Source : Hartline et al.1956)

In the top record of Figure 2.10, one strand which represents one ommaditium indicated by “A” was illuminated by itself at an intensity that elicited the discharge of 53 impulses in the period of the 1.5 seconds. In the bottom record, other ommaditium indicated by “B” was illuminated by itself at an intensity that elicited the discharge of 46 impulses in 1.5 seconds. In the middle record, both ommatidia were illuminated together, each at the same intensity as before; ommaditium “A” discharged 43 impulses, ommaditium “B” discharged 35 impulses, in 1.5 seconds (Hartline et al.1956). The

decrease in impulse frequency for each ommatidia was named as a magnitude of the inhibition generated by neighbour ommatidia on the recorded ommatidia.

Experiments similar to that illustrated in Figure 2.10 make it possible to show quantitatively how the amount of inhibition exerted on a receptor varies with the degree of activity of a neighbour receptor unit. The mutual interaction of two receptors can be analysed by stimulating each of them at different intensities separately and in combination. The result of such an experiment is shown in Figure 2.11. In this experiment, the frequencies of discharge of each of two ommatidia were measured, for various intensities of illumination, when each was illuminated alone and when both were illuminated together. The decrease in the frequency of discharge of each has been plotted against the frequency of the concurrent discharge of the other receptor unit. Figure 2.11(a) shows the amount of inhibition exerted upon ommatidium B by ommatidium A, as a function of the degree of activity of A; the Figure 2.11(b) shows the converse effect upon A of the activity of B. Both sets of points were well fitted with straight lines. In each case there was a fairly distinct threshold for the inhibition; each ommatidium had to be brought to a level of activity of 8 or 9 impulses per second before it began to affect the discharge of the other. Above this threshold, the frequency of discharge of B was decreased by 0.15 impulse per second for each increment of 1 impulse per second in the level of activity of A; the corresponding coefficient of the inhibitory action in the reverse direction (A acted on by B) was 0.17, The results that were established experimentally are summarized in the following mathematical expression:

$$r_A = e_A - \beta_{AB}*(r_B - r_B^0) \qquad (2.1)$$

$$r_B = e_B - \beta_{BA}*(r_A - r_A^0) \qquad (2.2)$$

where :

- $r_A$ and $r_B$ are after inhibition mechanism impulses of ommaditium “A” and “B” respectively,
- $e_A$ and $e_B$ are individual impulses of ommaditium “A” and “B” respectively
- $\beta_{AB}$ is inhibitory coefficient of ommaditium “B” on ommaditium “A”

  $\beta_{BA}$ is inhibitory coefficient of ommaditium “A” on ommaditium “B”
- $r_A^0$ and $r_B^0$ are threshold frequencies of ommaditium “A” and “B” respectively.

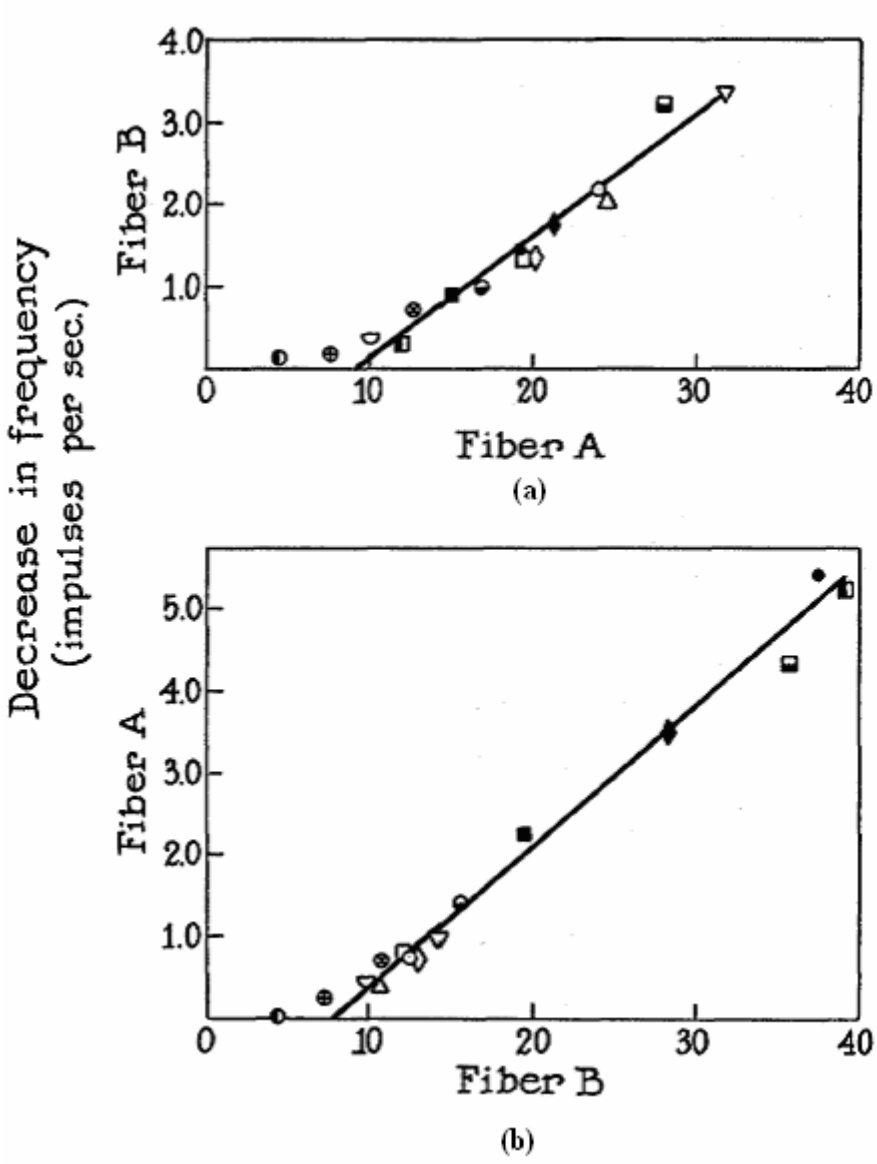


Figure 2.11. Mutual inhibition of two receptor units in the lateral eye of Horseshoe Crab (a) Response of fiber A (b) Response of fiber B (Source: Hartline et al.1956)

As mentioned before, the inhibition exerted mutually among the ommaditia of the lateral eye of Horseshoe Crab depends on the degree of activity of each of these receptor units. It also depends on the number and locations of units interacting (Hartline et.al 1957). When more than two receptor units are activated in an Horseshoe Crab eye, impulse frequency of each receptor unit was determined by a set of simultaneous relationship that states not only external light distribution over these receptor units but

also the magnitude of mutual inhibitory influences among them and the way in which the influences from many elements combine to affect the activity of each one.

When three receptor units (A, B, C) are active, three simultaneous equations will be required to determine the responses of each receptor unit. Each equation must contain two inhibitory terms as ;

$$r_A = e_A - [\beta_{AB}*(r_B - r_{AB}^{0}) + \beta_{AC}*(r_C - r_{AC}^{0})] \quad (2.3)$$

$$r_B = e_B - [\beta_{BC}*(r_C - r_{BC}^{0}) + \beta_{BA}*(r_A - r_{BA}^{0})] \quad (2.4)$$

$$r_C = e_C - [\beta_{CA}*(r_A - r_{CA}^{0}) + \beta_{CB}*(r_B - r_{CB}^{0})] \quad (2.5)$$

where :

- $r_A$, $r_B$ and $r_C$ are after inhibition mechanism impulses of ommaditium "A" ,"B" and "C" respectively,
- $e_A$ ,$e_B$ and $e_C$ are individual impulses of ommaditium "A" , "B" and "C" respectively
- $\beta_{AB}$ , $\beta_{BA}$ , $\beta_{AC,}$ $\beta_{CA,}$ $\beta_{BC}$ , $\beta_{CB}$ are inhibitory coefficients among three ommaditiums A, B ,C.
- $r_A^{0}$ $r_B^{0}$ and $r_C^{0}$are threshold frequencies of ommaditium "A" ,"B" and "C" respectively.

These equations can be extended to describe the impulse frequency of "n" number of interacting receptor units as follows :

$$r_p = e_p - \sum_{j=1}^{n} \beta_{pj} * (r_j - r_{pj}^{0}) \quad (2.6)$$

where ; p = 1,2,3,…….n ; $j \neq p$ ; $r_j > r_j^{0}$

Although there is no observation about excitatory interaction between receptor units of Horseshoe Crab and it is believed that all physiological interaction in the eye of Horseshoe Crab is purely inhibitory, studies about human sensory and neural system

proved that self-excitatory influences are also possible in more complex systems. When self-excitatory influences are considered the Equation 2.6 transforms into following form:

$$r_p = e_p + \alpha_p * e_p - \sum_{j=1}^{n} \beta_{pj} * (r_j - r_{pj}^{\ 0}) \qquad (2.7)$$

where ; α is the self-excitatory coefficient of receptor unit.

$$r_p = e_p + \alpha_p * e_p - \sum_{j=1}^{n} \beta_{pj} * r_j \qquad (2.8)$$

Therefore, for simplicity it is assumed that all threshold frequencies are zero and Equation 2.7 turns into Equation 2.8.

# CHAPTER 3

# THE EFFECTS OF LATERAL INHIBITION

As a result of applying lateral inhibition mechanism to any sensory network, some effects are observed in the output of network. Especially at some level of human nervous and sensory systems, lateral inhibition and its effects play an important role. According to the inhibitory or excitatory characteristic of the lateral interactions the effects of lateral inhibition can vary. These effects can be divided into three classes:

I. Contrast enhancement effect
II. Funnelling effect
III. Two point discrimination effect

## 3.1. Contrast Enhancement Effect

Figure 3.1 is the illustration of contrast enhancement effect. The horizontal direction represents sensor numbers in a distributed sensory network. The vertical direction represents magnitude. It can be seen that the discontinuity in the input is exaggerated in the output with lateral inhibition. In the visual system the contrast enhancement effect can be clearly seen.

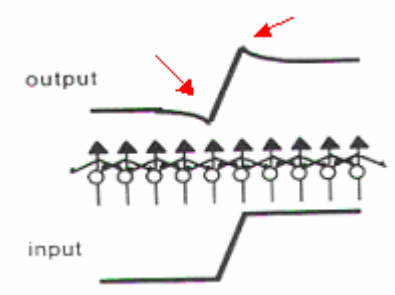


Figure 3.1 Contrast Enhancement
(Source: Brooks, 1988)

### 3.1.1. The Visual System

The human visual system can be regarded as consisting of two parts. The eyes act as image receptors which capture light and convert it into signals which are then transmitted to image processing centres in the brain. These centres process the signals received from the eyes and build an internal "picture" of the scene being viewed. Processing by the brain consists, partly, of simple image processing and partly of higher functions which build and manipulate an internal model of the outside world. Although the division of function between the eyes and the brain is not clear-cut, it is useful to consider each of the components separately.

### 3.1.2. The Eye

The structure of the human eye is analogous to that of a camera. The basic structure of the eye is displayed in Figure 3.2.

- The *cornea* and *aqueous humour* act as a primary lens which perform crude focusing of the incoming light signal.
- A muscle called the *zonula* controls both the shape and positioning (forward and backwards) of the eye's *lens*. This provides a fine control over how the light entering the eye is focused.
- The *iris* is a muscle which, when contracted, covers all but a small central portion of the lens. This allows dynamic control of the amount of light entering the eye, so that the eye can work well in a wide range of viewing conditions, from dim to very bright light. The portion of the lens not covered by the iris is called the *pupil*.
- The retina where contrast enhancement effect observed provides a photo-sensitive screen at the back of the eye, which incoming light is focused onto. Light hitting the retina is converted into nerve signals.
- A small central region of the retina, called the *fovea*, is particularly sensitive because it is tightly packed with photo-sensitive cells. It provides very good resolution and is used for close inspection of objects in the visual field.
- The optic nerve transmits the signals generated by the retina to the vision processing centres of the brain.

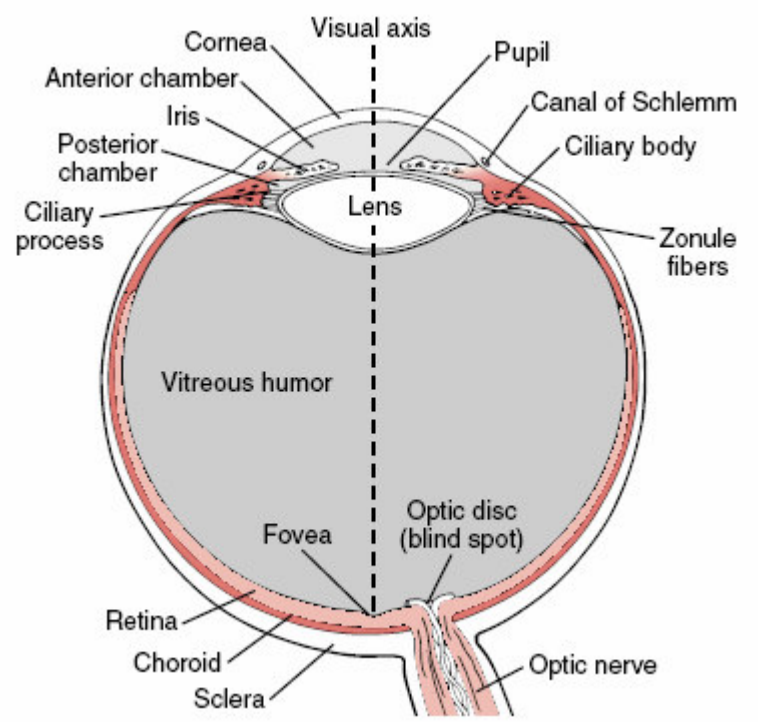


Figure 3.2. Major parts of human eye

(Source: Meiss, 1999)

### 3.1.3. The Retina

The retina is composed of a thin layer of cells lining the interior back and sides of the eye. Many of the cells making up the retina are specialised nerve cells which are almost similar to the tissue of the brain. Other cells are light-sensitive and convert incoming light into nerve signals which are transmitted by the other retinal cells to the optic nerve and from there to the brain. There are two general classes of light sensitive cells in the retina; rods and cones. Rod cells are very sensitive and provide visual capability at very low light levels. Cone cells perform best at normal light levels. There are roughly 120 million rod cells and 6 million cone cells in the retina. There are more rods than cones because they are used at low light levels and more of them are required to gather the light.

### 3.1.4. Retinal Circuitry

Although there are some 120 millions rods and 6 millions cone cells in the retina, there are less than a million optic nerve fibres which connect them to the brain. This means that there can not be a single one-to-one connection between the photoreceptors and the nerve fibres. The number of receptors connecting to each fibre is location dependent. In the outer part of the retina, as many as 600 rods are connected to each nerve fibre, while in the fovea there is an almost one-to-one connection between cones and fibres. In addition to the rods and cones there are a number of other cell types whose function is to gather and process the information produced by the photoreceptors.

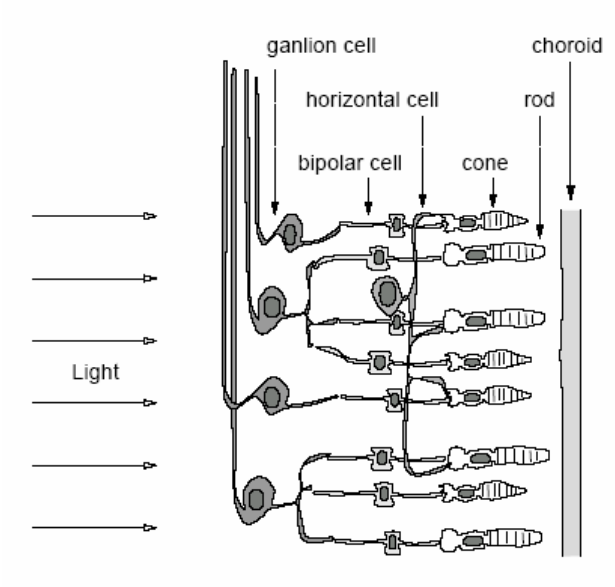


Figure 3.3. The arrangement of cells in the retina
(Source: WEB_2 2005)

The mechanism by which a neural cell can pass information to multiple cells is through horizontal and amacrine cells (Figure 3.4). A receptor cell can directly pass information to a bipolar cell, but in order to pass information to other bipolar cells, that electrical signal is also passed via horizontal cells. The bipolar cells send electrical pulses to multiple ganglia through similar cells known as amacrine cells. The ganglion cells serve as terminators for the nerve fibres connecting to the brain. Throughout most of the retina, bipolars gather signals from several receptors while in the fovea there is

usually one for each receptor. The horizontal cells connect adjacent receptors and amacrine cells link multiple ganglions. The major three types (receptor, bipolar and ganglia) of neural cells send excitatory signals, and the horizontal and amacrine cells send inhibitory signals.

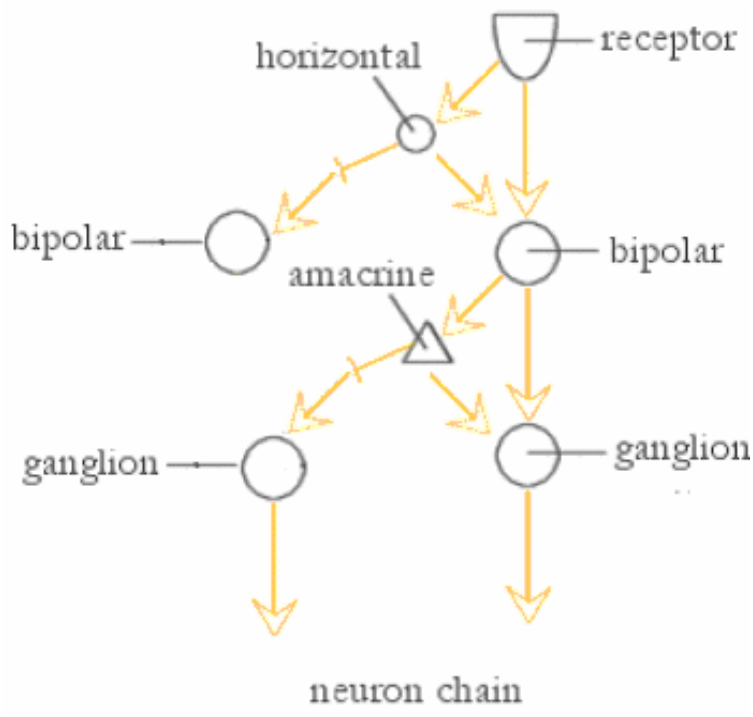


Figure 3.4. Neural pathway of visual stimulus in the retina

Figure 3.3 shows the arrangement of these cells in the retina. Notice that the arrangement is counter intuitive, with light passing through the connecting "circuitry" before falling on the light sensitive receptors.

### 3.1.5. Lateral Inhibition and Vision

The complexity of the connections in Figure 3.3 and the neural structure displayed in Figure 3.4 indicate that the retina is capable of some quite complex signal processing operations. In addition to the inhibitory nature of horizontal cells and amacrine cells, excitatory effects of biopolar cells and ganglion cells make the lateral inhibition a common form of processing which takes place in the retina.

All neural cells have their own rate of firing, known as the spontaneous rate of firing, when they are not stimulated. In the case of excitatory cells, some proportion of their firing rate is added to a synapsed cell. The proportion that is added to synapsed cell is dependant on the "weight" of the neural cell. For example, if some excitatory bipolar cell with a weight of 0.5 has a firing rate of 20, it will add 10 to the spontaneous firing rate of all the neural cells that it sends information to. The weight of a neural cell can also be negative, which will add a negative number, or subtract from the spontaneous firing rates of the cells that are synapsed to it. It is important to keep in mind at this point, that excitatory and inhibitory cells do not affect the firing rates of the neural cells that pass information to it. Excitatory and inhibitory signals are only passed one way down the neural chain.

When a local section of the retina is excited, the cells on the excited part of the retina do not just signal to the visual processing centres of the brain. They also send signals to neighbouring cells whose effect is to diminish or inhibit the effect of any excitation taking place there. Figure 3.5 shows the effects of a very simple model for lateral inhibition. Parts (a) and (b) of the figure show the sensory system operating without the effects of inhibition. In part (a) a uniform stimulation is applied to an array of sensors. The result is a constant level of output from the sensors. In part (b), the level of stimulation is not continuous it shows a sudden increase. The result has also sudden increase simultaneously. Part (c) of the figure shows the effect when inhibition is introduced to the system. As well as outputting its signal, each sensor has an inhibitory effect on its two neighbours. The resulting sensor output is quite similar to (b), but at the boundary between the two levels of excitation, the difference in the output is accentuated. In image processing, treating signals in this way is known as edge enhancement.

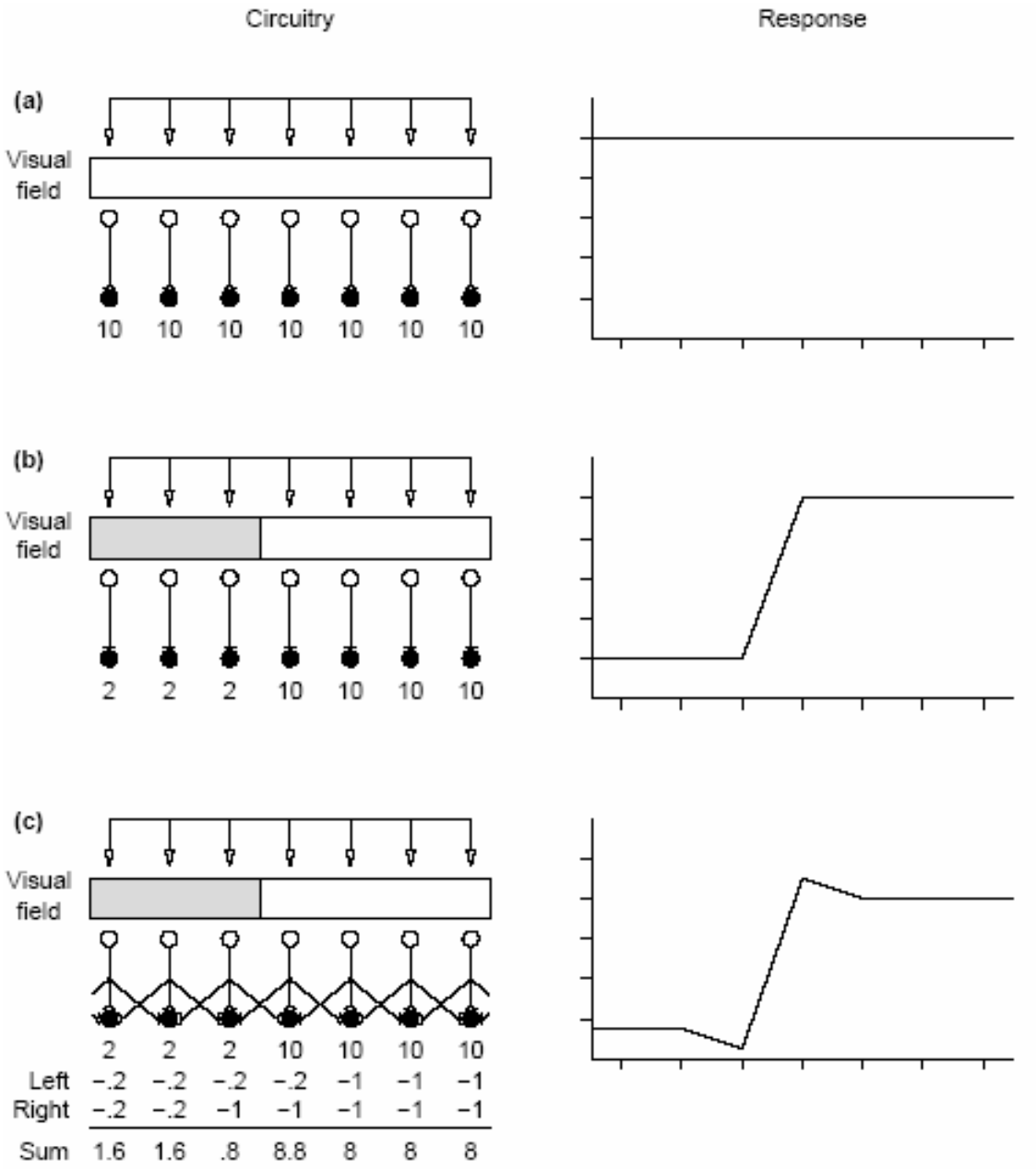


Figure 3.5. The effects of lateral inhibition on edge enhancement

Different from the interactions which are displayed in Figure 3.5 and described above, the signals transmitted in retinal circuitry can be inhibitory and excitatory depending on the transmitter cell types. In case of visual stimulation influenced by excitatory and inhibitory interaction, the output of the network becomes different. Although the edge enhancement effect occurs as a result of inhibitory interactions shown in Figure 3.5, contrast enhancement effect can not be observed. When excitatory

interactions are inserted in the neural circuitry the contrast difference between the stimulation is increased. This effect can be seen in figure 3.6.

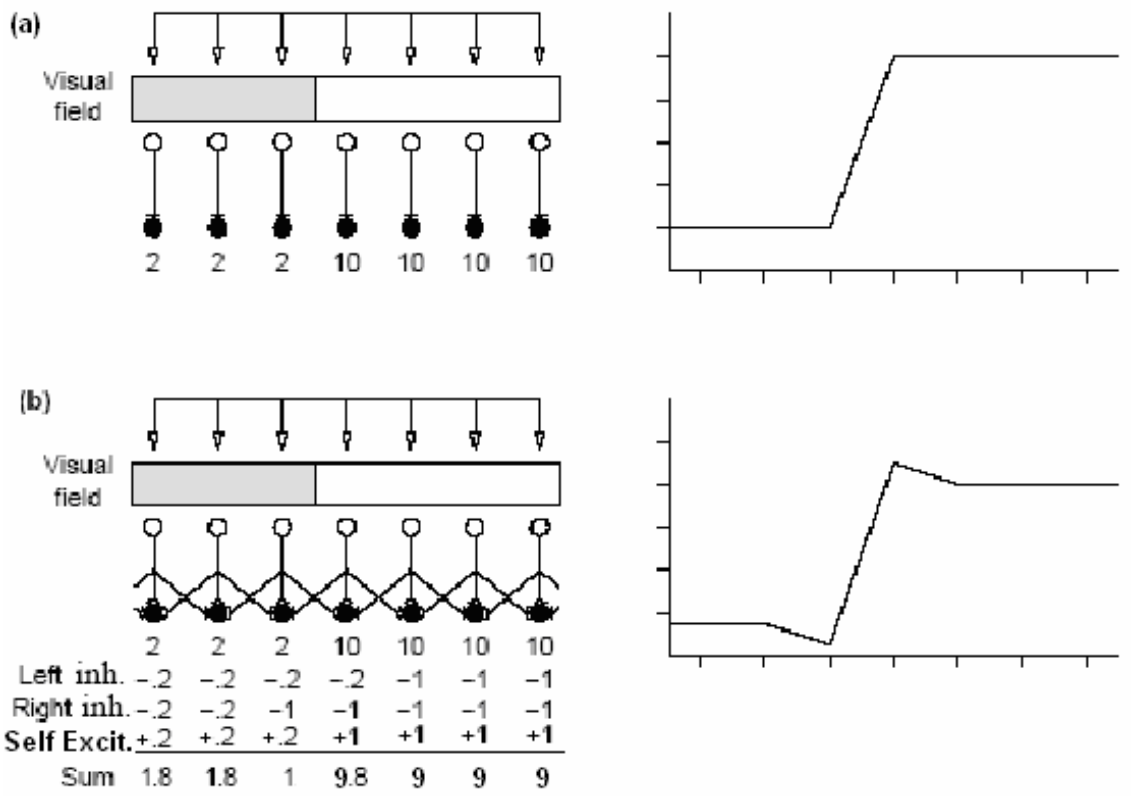


Figure 3.6. The effects of lateral inhibition on contrast enhancement.

A good visual illustration that displays the contrast enhancement effect can be seen in Figure 3.7. It is a visual illusion which is known as Kaniza Triangle. Although the visual stimulus and its retinal projection is just three pie shaped figures, an imaginary triangle is perceived on the top of the three circles. As a result of the contrast enhancement effect of the lateral inhibition mechanism, a thin illusory lines are perceived at each border of the differing colours. In addition to that, contrast enhancement effect makes the triangle which are bordered by illusory lines appear brighter than its background.

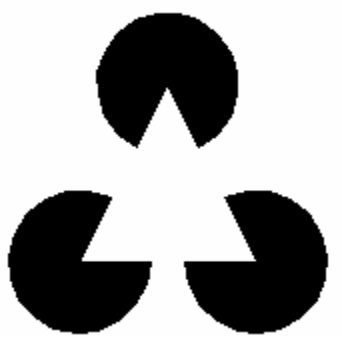

Figure 3.7. Kaniza triangle

## 3.2. Funnelling Effect

Funnelling effect is illustrated in Figure 3.8. Even though the external stimulus has a large effect on the sensory organ or receptor, the response of the network funnelled into sharp peak. This effect is efficient when the sensory information transferred to a processing center after via multiple relay stations. The funnelling effect can be clearly seen in auditory pathway.

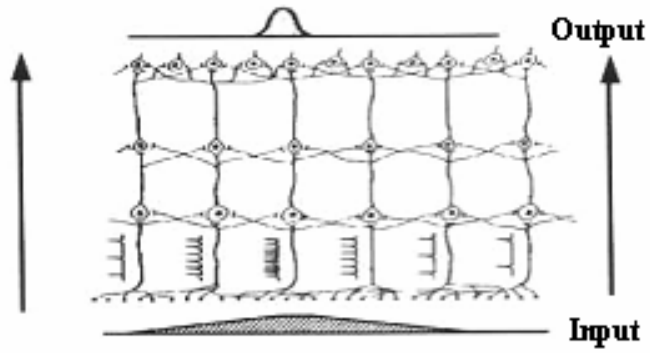


Figure 3.8. Illustration of funnelling effect
(Source: Brooks 1988)

### 3.2.1. Auditory Pathway

The central auditory pathways extend from the inner ear to the cerebral cortex. Although audition is classified as a member of sensory system, auditory pathway differs

from the somatosensory and visual pathways in that there is no large direct pathway from sensors to the cortex. Rather, information ultimately reaching the auditory cortex undergoes significant reorganization as it passes through the auditory cortex (Moore, 1997). Along the complex and highly ordered pathway a series of nerve cells are operated to process and relay auditory information which is encoded in the form of nerve impulses. A general conclusion reached from studies on the anatomic and chemical composition of the auditory pathway is that inhibition plays an extremely important role at all levels of the system in shaping the exquisitely precise responses of auditory neurons ( Jackler et al. 1994).

### 3.2.2. The Ear

The ear can be divided into three subparts such as outer ear, middle ear and inner air and each part has different task. Outer or external ear has ability to introduce sound in a specific direction and has a minor role in amplification of sound. Middle ear acts to transmit changes in air pressure (sound) from the outer ear canal to inner ear and increases the efficiency of sound transmission. It converts high amplitude, low force input into low amplitude, high force output. Inner ear is thought as the beginning of auditory pathway because transduction of external stimulus to neural information takes place in it. The sound waves directed by outer ear and amplified by middle ear create a motion in fluid of inner air (scala vestibuli) and this motion causes a displacement on the basilar membrane which is a part of inner air (Figure 3.9).

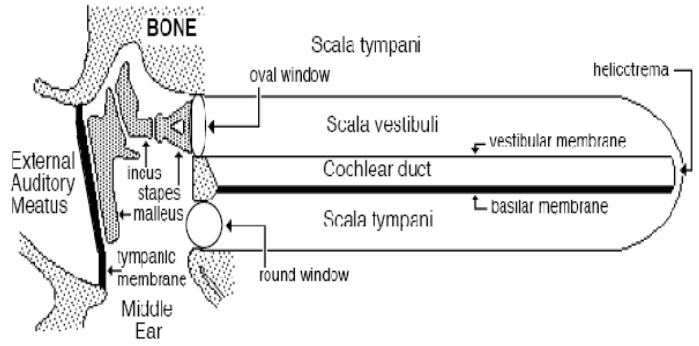


Figure 3.9. Simple anatomic illustration of ear
(Source: Moore, 1997)

### 3.2.3. Basilar Membrane

The basilar membrane varies in width, increasing from base to apex, and this causes differences in stiffness of the basilar membrane. Neighbouring parts of the membrane vibrate relatively independently of each other, and so each point along the membrane has a particular resonant frequency to which it will respond maximally (Figure 3.10).

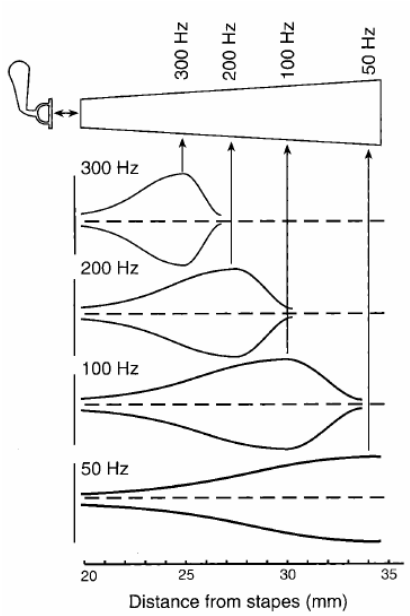


Figure 3.10 Frequency Distribution of Basilar Membrane
(Source : Moore, 1997)

These frequencies are high at the base, and decrease logarithmically towards the apex as shown in Figure 3.10. This mechanism gives the ear an ability to distinguish different frequencies. As a result of the motion of basilar membrane, the hair cells which are connected to basilar membrane transduct the external stimuli to neural information.

### 3.2.4. Lateral Inhibition and Audition

The high frequency resolution of the ear suggest that only about a dozen hair cells associated with each distinguishable frequency (Figure 3.11). It is hard to conceive of a mechanical resonance of the basilar membrane that sharp (McGutin, 1993). There are some mechanisms that sharpen the response of the basilar membrane as illustrated in Figure 3.12.

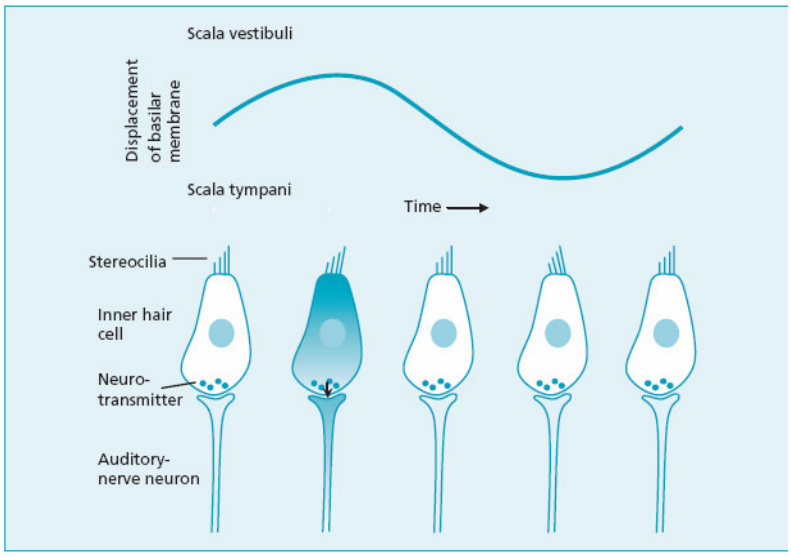


Figure 3.11.Relation between basilar membrane and hair cells

(Source: Plack ,1999)

Several of the proposed mechanisms have the nature of lateral inhibition on the basilar membrane. One way to sharpen the pitch perception would be bring the peak of the excitation pattern on the basilar membrane into greater relief by inhibiting the firing of those hair cells which are adjacent to the peaks. Since nerve cells obey an "all-or-none" law.

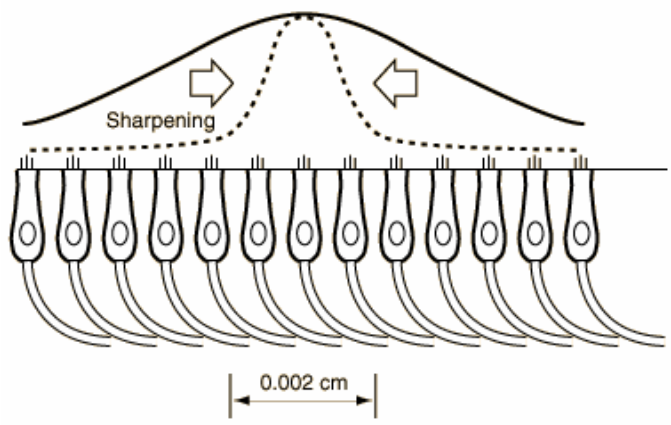


Figure 3.12 Illustration of sharpening

(Source: WEB_3 2005)

When receiving the appropriate stimulus and then drawing energy from the metabolism to recharge before firing again, one form the lateral inhibition could take is the inhibition of the recharging process since the cells at the peak of the response will

be drawing energy from the surrounding fluid the most rapidly. Inhibition of the lateral hair cells could also occur at the ganglia, with some kind of inhibitory gating which lets through only those pulses from the cells which are firing the most rapidly. It is known that there are feedback signals from the brain to the hair cells, so the inhibition could occur by that means.

After the transduction of external stimulus into neural code in the inner ear the neural information continuous its ascending way to the cortex. During the auditory pathway there are stations that are devoted primarily to processing auditory information (Figure 3.13). The first processing or relay station is the cochlear nucleus. The auditory signal or information is then passed to the superior olivary complex. Further up the auditory pathway are the lateral leminiscus and the inferior colliculus. The auditory information is passed to the primary auditory cortex via the medical geniculate body of the thalamus. Each relay station contains different types of neurons with varying properties that process the auditory information and one receiver neuron can be related more than one transmitter neuron. As a result of this kind of relation between neurons causes excitatory or inhibitory interactions depending on the type of chemical released into the synapse. Some type of chemical such as acetylcholine (ACh) makes the interaction excitatory and some type of chemical such as gamma-aminobutyric acid (GABA) makes the interaction inhibitory.

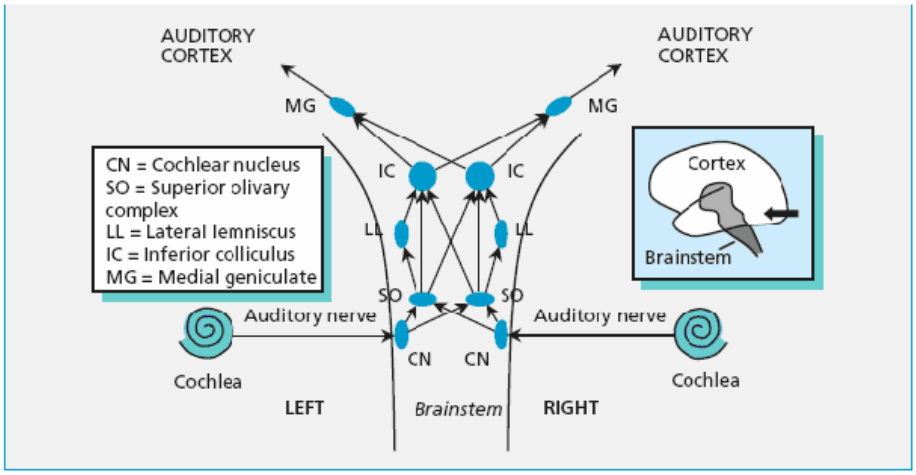


Figure 3.13.Main relay stations in the ascending auditory pathway

(Source: Plack ,1999)

The clear evidence of this type of lateral inhibition can be seen on the threshold tuning curves of the external stimulus (Figure 3.14). Auditory tuning curves or frequency threshold curve, maps the threshold boundary of a neuron or fiber. The frequency of maximum sensitivity, or characteristic frequency, is the neuron's most sensitive frequency. Along the auditory pathway tuning curves get sharper after each relay station.

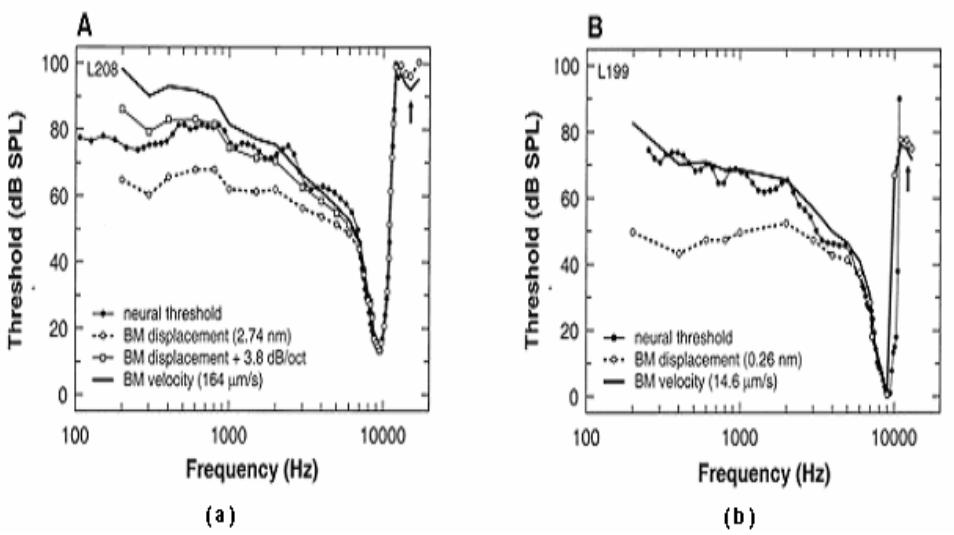


Fig. 3.14. (a) Frequency tuning of responses to tones of Basilar membrane (b) frequency tuning of responses to tones of auditory nerve fibers with similar characteristic frequency. (Source: Narayan 1984)

It is clearly seen in Figure 3.14 the" v" shape of tuning curve gets sharper for auditory nerve fibre which is coming after from basilar membrane in auditory pathway. The Q value is calculated by dividing the best frequency (in Hz) of the tuning curve by the width of the tuning curve 10 decibels up from the most sensitive threshold indicates that the quality of the tuning curve can range from 1 to 4 in the auditory nerve but in cochlear nucleus which is the next step after the auditory nerve in the auditory pathway Q value can be as high as 20.

## 3.3. Two Point Discrimination Effect

Two point discrimination is an another effect of lateral inhibition mechanisms. This effect gives the network ability to distinguish two closely placed stimuli as two

discrete points rather than as one fused point. This effect is generally used in human somatosensory system. When static pressure applied to skin at two points a few millimetre apart the output is blurred without lateral inhibition mechanism but with lateral inhibition each stimulus are clearly distinguishable. The illustration of two point discrimination effect can be seen in Figure 3.15.

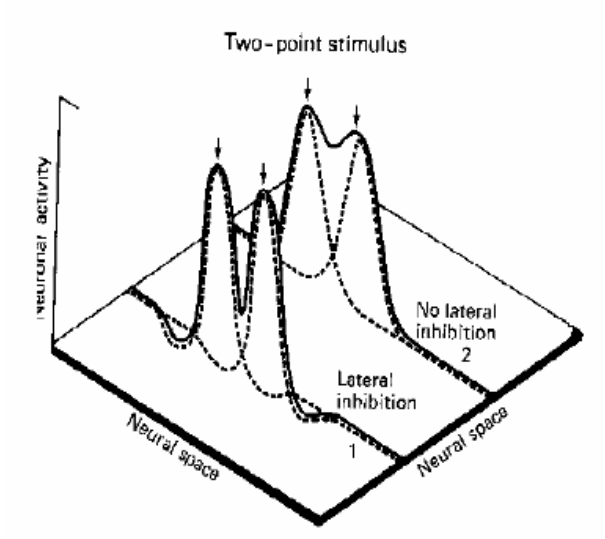


Figure 3.15. Schematic illustration of two point discrimination effect
(Source : Brooks, 1988)

## 3.3.1. Somatosensory System

The somatic sensory system allows us to perceive and recognize objects through touch. This system is different from other sensory systems for two reasons. One, the receptors for somatic sensibility are not restricted to a small, well –delineated organ like the eye for vision or the cochlea for hearing, but are spread throughout the body. For this reason the somatic sensibilities are called skin or the body senses. Second, the sensations mediated by the somatic sensory system are remarkably diverse; they include not only the four relatively elementary sub-modalities - touch, pressure, temperature and pain - but also various compound sensations such as vibration, itch and tickle that are achieved by combining elementary sub-modalities in different ways. Normal human somatic sensibility is usually subdivided into 4 major types;

(1) Discriminatory tactile sensibility (fine touch and pressure)

(2) Position sense (static position and kinesthesia)

(3) Pain (slow and fast)

(4) Temperature sense (warm and cold)

To achieve all somatic sensibilities there are specific receptors (Figure 3.16) for each sub-modality. For example, Meissner's corpuscles mediate superficial touch and Pacinian corpuscles mediate vibration.

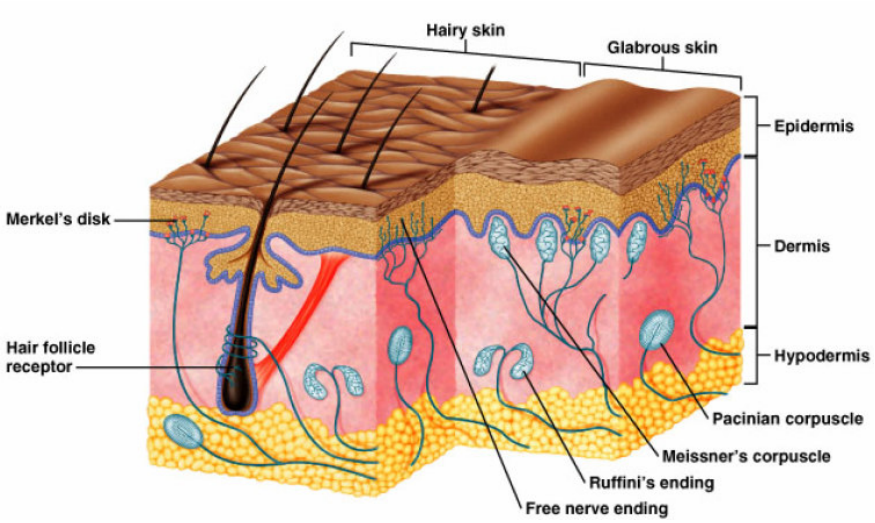


Figure 3.16 Section of human skin

(Source:Murphy, 2002)

## 3.3.2. Somatosensory Pathway

Many aspects of tactile sensibility and position sense are carried by the dorsal column medial lemniscal system and are therefore also called dorsal column–medial lemniscal modalities. Large myelinated afferent fibers from these receptors in skin, subcutaneous tissues and deep tissue enter the spinal cord via the dorsal roots. Each axon divides and sends a long ascending branch into the dorsal columns to synapse in the medulla with cells in the dorsal column nuclei. Axons of second- order sensory cells in the dorsal column nuclei cross the midline in the medulla. These axons then ascend the brain stem on the opposite side as the medial lemniscus and from synapses with the cells in the ventral posterior lateral nucleus of the thalamus (Figure 3.17) and as a last step the third - order neurons in the thalamus send axons to the cerebral cortex.

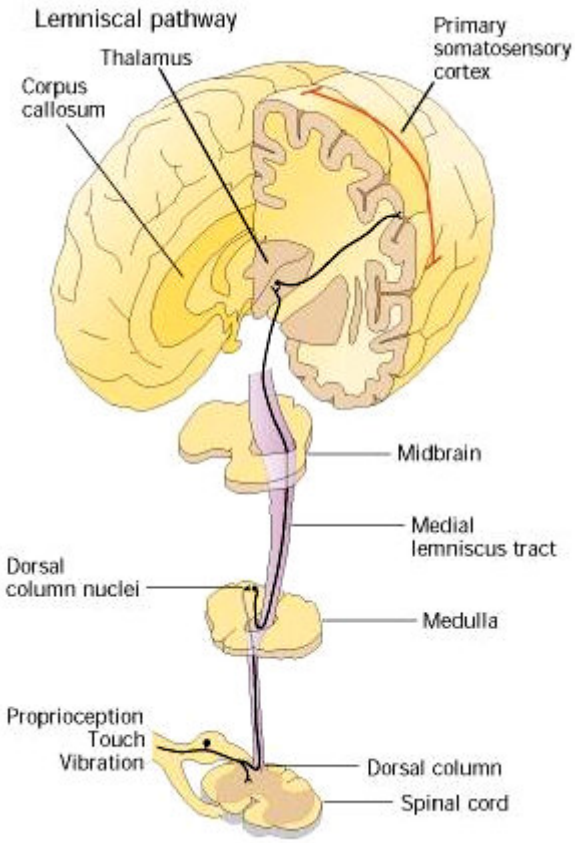


Figure 3.17. Somatosensory pathway

(Source: WEB_4 2005)

According to the anatomical plan of the somatosensory pathway illustrated in Figure 3.17, a pathway consists of a series of relay points up to the cortex. At each relay nucleus the principal relay cells receive synaptic input from many afferent fibres; each afferent cell ends on many relay cells. In addition to relay cells, the afferent fibers activate both excitatory and inhibitory interneurons. As a result, the sensory information can be processed by passage from the principal neurons of one nucleus to those of the next. In some nuclei the information may be transformed into a new, more abstract, pattern of activity; in others, the afferent message will ascend to the next level without change.

### 3.3.3. Lateral Inhibition and Somatosensory System

The neurons in the somatic sensory system are not silent but spontaneously active. Sensory stimuli therefore act to modulate ongoing neural activity in central

nuclei and in cerebral cortex. Moreover, a given cell's activity can not be modulated by stimuli applied at any point on the body surface. Rather, for each cell there is a specific area of the skin that can alter its firing rate. The area is called a 'receptive field' of the cell (Figure 3.18).

The size of the receptive field varies, corresponding to the intensity of the receptors in the body surface. The areas of the skin that are most sensitive to touch and therefore have the greatest cortical representation are the tips of the fingers and tongue. They have the smallest receptive fields and the largest number of receptive fields per unit area of skin. There are also more neural innervations in these areas and it causes more sensibility and ability to distinguish two close stimulus.

According to the receptive field theory, two stimuli which are applied to separate positions on the skin sets up two excitatory gradients of activity at every relay point in the somatic sensory system. The activity in each population of cells have a discrete peak. The inhibitory surround sharpens each peak and further enhances the distinction between two peaks.

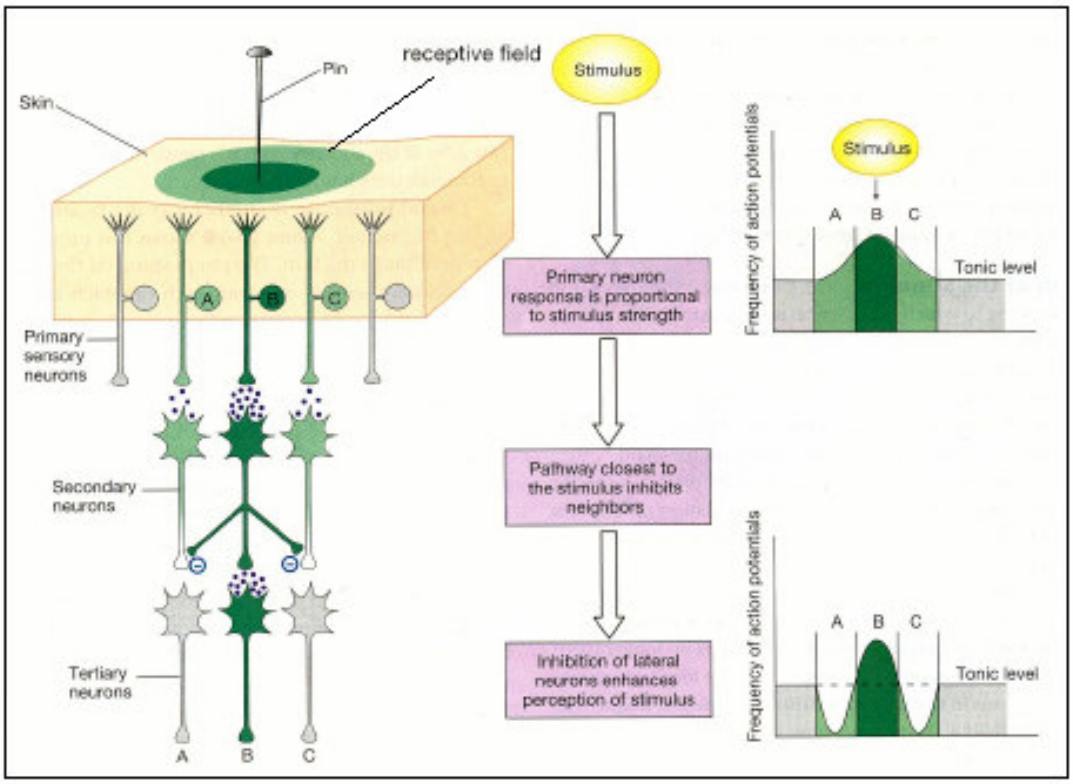


Figure 3.18. Schematic illustration of receptive field and neural interactions (Source: Paré, 2001)

When a single point stimulus applied to the skin a number of touch receptor activate and produce impulses in each of several first order activated afferent fibers. These afferent fibers provoke a group of cells in dorsal column nucleus and those cells activate another group of cells in the thalamus which provoke a group cells in the cortex. At each level the cells that discharge impulses are limited to restricted zone by two factors;

1. Excitatory anatomical connections
2. Lateral inhibition

When a two point stimuli applied to the skin each point sets up a gradient of activity at each level in the nervous system. Each stimulus excites a set of cells that have a receptive field with central excitatory zone surrounded by a weaker excitatory zone (Figure 3.19). The weaker excitatory zone is depressed by the inhibitory surround. When two stimuli are brought close together the surround inhibitions of each field in the neurons activated in the area of the skin between the two stimuli are summated. This summation of inhibition retards the fusion of the excitatory zones which are set up by the two stimulus. Therefore this summation preserves peaks of activity at the cortical level and enhances the contrast between the two points.

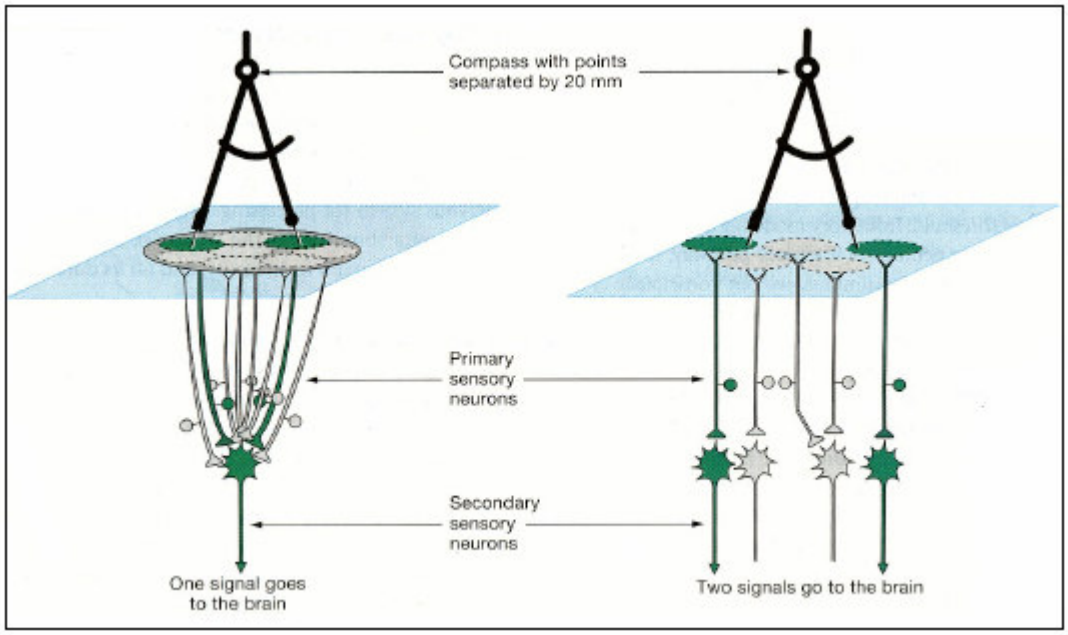


Figure 3.19 Effect of receptive field size on two point discrimination

(Source: Paré, 2001)

# CHAPTER 4

# EXPERIMENTAL SETUP

## 4.1. Experimental Setup

To observe the effects in the human sensory and nervous systems as a result of lateral inhibition mechanism two experimental setups were built. Each experimental setup consists of a light source and a sensory array with several photosensitive sensors such as light dependent resistors (LDR) or photodiodes because of their low costs. At the beginning, light dependent resistors were used in the experimental setup, which were later replaced by photodiodes to get better results.

In the first setup (Figure 4.1) there is a board contains several photosensitive sensors. These sensors were stimulated by a pair of point light sources (Light Emitting Diodes) whose position in space could be adjusted as seen on the left-hand side of the Figure 4.1.

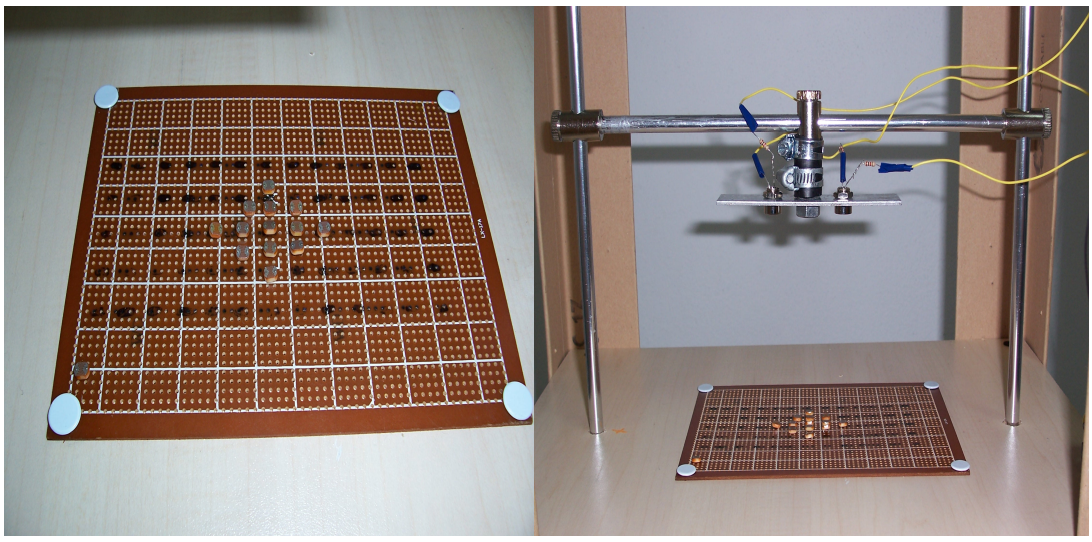

Figure 4.1 A photo showing first experimental setup.

The second experimental setup consists of a light source; 12V / 20W halogen lamp and a sensory array of several photosensitive sensors. The light source and photosensitive sensory array were placed in a frame which was constructed by FlexLink 44x44 aluminium profiles. This frame stabilized the sensory array and gave the light source an ability to move in three dimensions (Figure 4.2(a)). To separate the experimental setup from ambient light and to reduce noise level as minimum as possible the aluminium frame was placed into a box which was made of wood (Figure 4.2(b)).

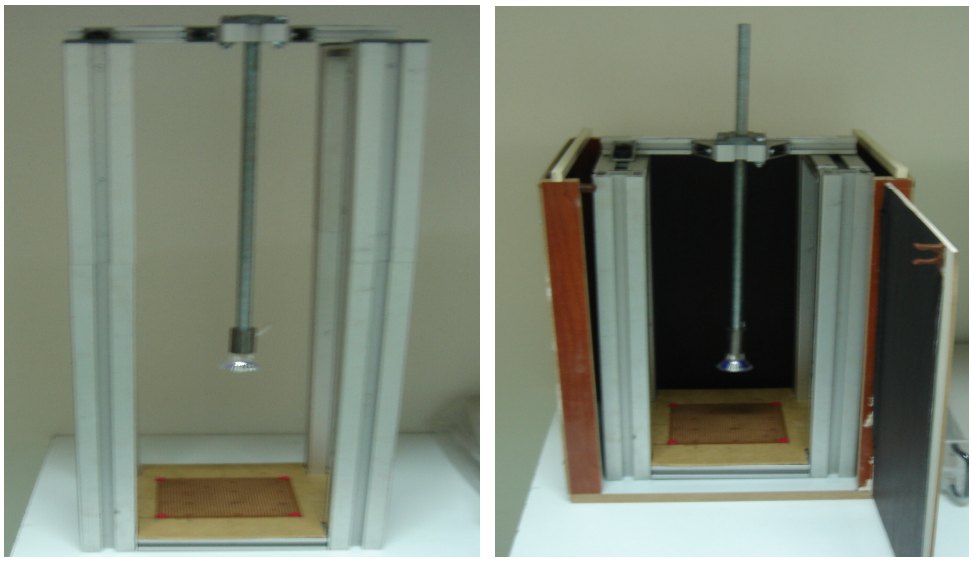

(a) (b)

Figure 4.2 A photo of second experimental setup.

Under the experimental conditions described above, the sensors were expected to respond depending on the light intensity that falls on to the individual ones. These sensors were connected to a Pentium 4 PC over a multiplexer which was then interfaced with a Keithley 2750 datalogger instrument and this instrument was controlled via ExceLink software (Figure 4.3). Each sensor had an address and successive readings were made in turn, given a specific setup.

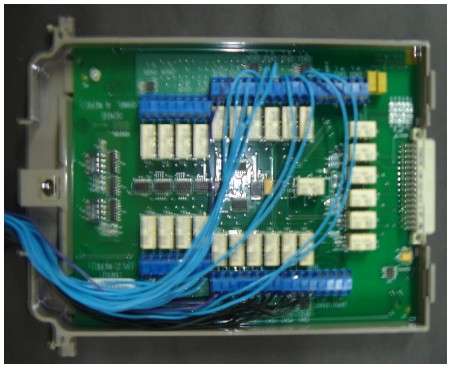

(a)


(b)

Figure 4.3 (a) photo showing connections of multiplexer (b) Keithley datalogger instrument.

These sensors were used in different configurations. So the input is light and output is the conductance of the LDRs and voltage of photodiodes. By changing the position of the light, various inputs and outputs were obtained.

## 4.2. Light Dependent Sensor (LDR)

Many materials have electrical resistance value that will change when light strikes the material. The light separates electrons from holes and allows both types of particles to move through the material and carry current. Because of the physical action, the effect is always that the material has high resistance in the absence of light, and the resistance drops when the material is illuminated.

The most common form of photoconductive cell is the cadmium sulphide cell, named after the material used as a photoconductor. This is often referred to as Light Dependent Resistor (LDR) .The cadmium sulphide is deposited as a thread pattern on an insulator, and since the length of this pattern affects the sensitivity, the shape is usually a zigzag line (Figure 4.4). The cell is then encapsulated in a transparent resin or encased in glass to protect the cadmium sulphide from contamination by the atmosphere.

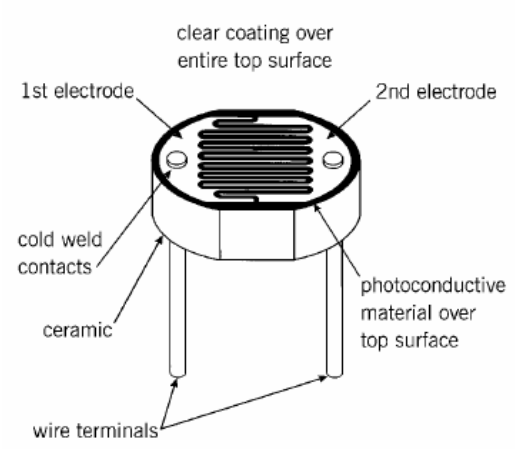


Figure 4.4 Schematic illustration of a light dependent resistor.
(Source: WEB_5 2005)

The cell is very rugged and can withstand a considerable range of temperatures, either in storage or in operation. The resistance range can also be considerable, particularly when a long track length of cadmium sulphide has been used, and this type of cell is one of the few devices that can be used with AC supply. Table 4.1 lists typical specifications for a popular type of cell, the ORP12. The peak spectral response of 610 nm corresponds to a colour in the yellow-orange region, and the dark resistance of 10MΩ will fall to a value in the ohms to kilo ohms region upon illumination. The sensitivity is not quoted as a single figure because the change of resistance plotted against illumination is not linear.

Table 4.1 Typical specification of a standard light dependent resistor
(Source:Sinclair, 2001)

| | |
|---|---|
| Peak Spectral Response | 610 nm |
| Cell Resistance at 50 lux | 2400 Ω |
| Cell Resistance at 1000 lux | 130 Ω |
| Dark Resistance | 10 M Ω |
| Typical Resistance Rise Time | 75 ms |
| Typical Resistance Fall Time | 350 ms |

## 4.3. Photodiode

Photodiodes are semiconductor light sensors that generate a current or voltage when the P-N junction in the semiconductor is illuminated by light. The term photodiode can be broadly defined to include even solar batteries, but it usually refers to sensors used to detect the intensity of light. There are many features of photodiodes such as excellent linearity with respect to incident light, low noise, wide spectral response and long life.

Figure 4.5 shows a cross section of a photodiode. The P-layer material at the active surface and the N material at the substrate form a PN junction which operates as a photoelectric converter. The usual P-layer for a Si photodiode is formed by selective diffusion of boron, to a thickness of approximately 1 μm or less and the neutral region at the junction between the P- and N-layers is known as the depletion layer. By controlling the thickness of the outer P-layer, substrate N-layer and bottom $N^+$ layer as well as the doping concentration, the spectral response and frequency response can be controlled.

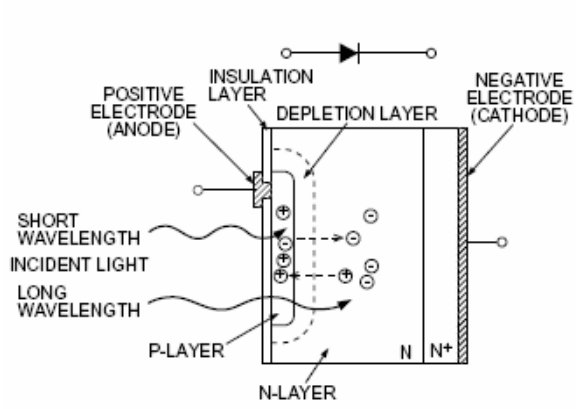


Figure 4.5 Illustration of cross section view of a photodiode
(Source: Sinclair, 2001)

When light strikes a photodiode, the electron within the crystal structure becomes stimulated. If the light energy is greater than the band gap energy $E_g$, the electrons are pulled up into the conduction band, leaving holes in their place in the valence band. These electron-hole pairs occur throughout the P-layer, depletion layer and N-layer materials. In the depletion layer the electric field accelerates these electrons

toward the N-layer and the holes toward the P-layer. Of the electron-hole pairs generated in the N-layer, the electrons, along with electrons that have arrived from the P-layer, are left in the N-layer conduction band. The holes at this time are being diffused through the N-layer up to the depletion layer while being accelerated, and collected in the P-layer valence band. In this manner, electron-hole pairs which are generated in proportion to the amount of incident light are collected in the N- and P-layers. This results in a positive charge in the P-layer and a negative charge in the N-layer. If an external circuit is connected between the P- and N-layers, electrons will flow away from the N-layer, and holes will flow away from the P-layer toward the opposite respective electrodes. These electrons and holes generating a current flow in a semiconductor are called the carriers.

## 4.4. Trilateration

Trilateration is a basic geometric principle that provides to find a location using relative positions of three or more known locations similar to triangulation. Unlike triangulation, which uses angle measurements (together with at least one known distance) to calculate the subject's location, trilateration uses the known locations of two or more reference points, and the measured distance between the subject and each reference point. To accurately and uniquely determine the relative location of a point in two-dimensional space, at least three circles are needed to pinpoint the location. In three-dimensional space, at least four spheres are needed.

Trilateration can be applied to many different areas, such as geographic mapping, navigation (e.g. GPS systems), and due to the progress in electronic distance-measuring it is preferred to triangulation.

The mathematical derivation of 2D trilateration is quite simple, in case of known exact position of three different receivers and distances between the receivers and target the exact position of the target can be determined. Figure 4.6(a) shows how trilateration works; where A, B, and C are beacons with known locations. From A’s signal, one can determine that the object should be located at the circle centred at A. Similarly, from B’s and C’s signals, it can be determined that the object should be located at the circles centred at B and C, respectively. Thus, the intersection of the three circles is the estimated location of the device. The preceding discussion has assumed an ideal

situation; however distance estimation always contains errors that will, in turn, lead to location errors. Figure 4.6(b) illustrates an example in practice. The three circles do not intersect in a common point. In this case, the maximum likelihood method may be used to estimate the device's location. Let the three beacons A, B, and C be located at $(x_A , y_A)$, $(x_B , y_B)$ and $(x_C , y_C)$, respectively. For any point $(x, y)$ on the plane, a difference function is computed as

$$\sigma_{x,y} = |\sqrt{(x-x_A)^2+(y-y_A)^2} - r_A| + |\sqrt{(x-x_B)^2+(y-y_B)^2} - r_B| + |\sqrt{(x-x_C)^2+(y-y_C)^2} - r_C|$$

where $r_A$ , $r_B$, and $r_C$ are the estimated distances to A, B, and C, respectively. The location of the object can then be predicted as the point $(x, y)$ among all points such that $\sigma_{x,y}$ is minimized.

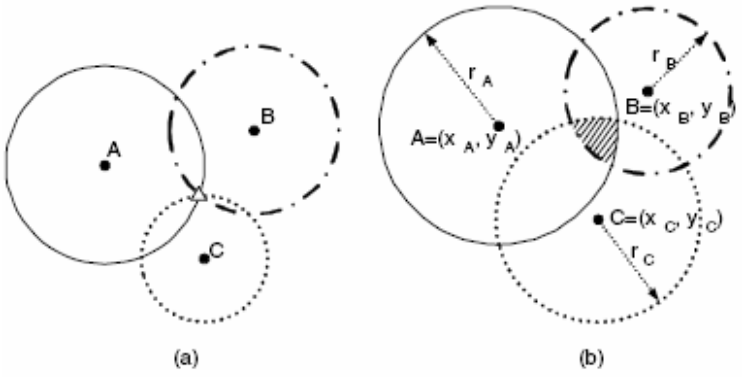


Figure 4.6 Trilateration method: (a) ideal situation; (b) real situation with errors.
(Source: Savvides, 2001)

When the trilateration expands into 3D space it becomes more complex. 3D-trilateration is also called as multilateration or hyperbolic positioning. Multilateration is commonly used in civil and military surveillance applications to accurately locate aircraft, vehicle or stationary emitter by measuring the time difference of arrival of a signal from the emitter at three or more receiver sites.

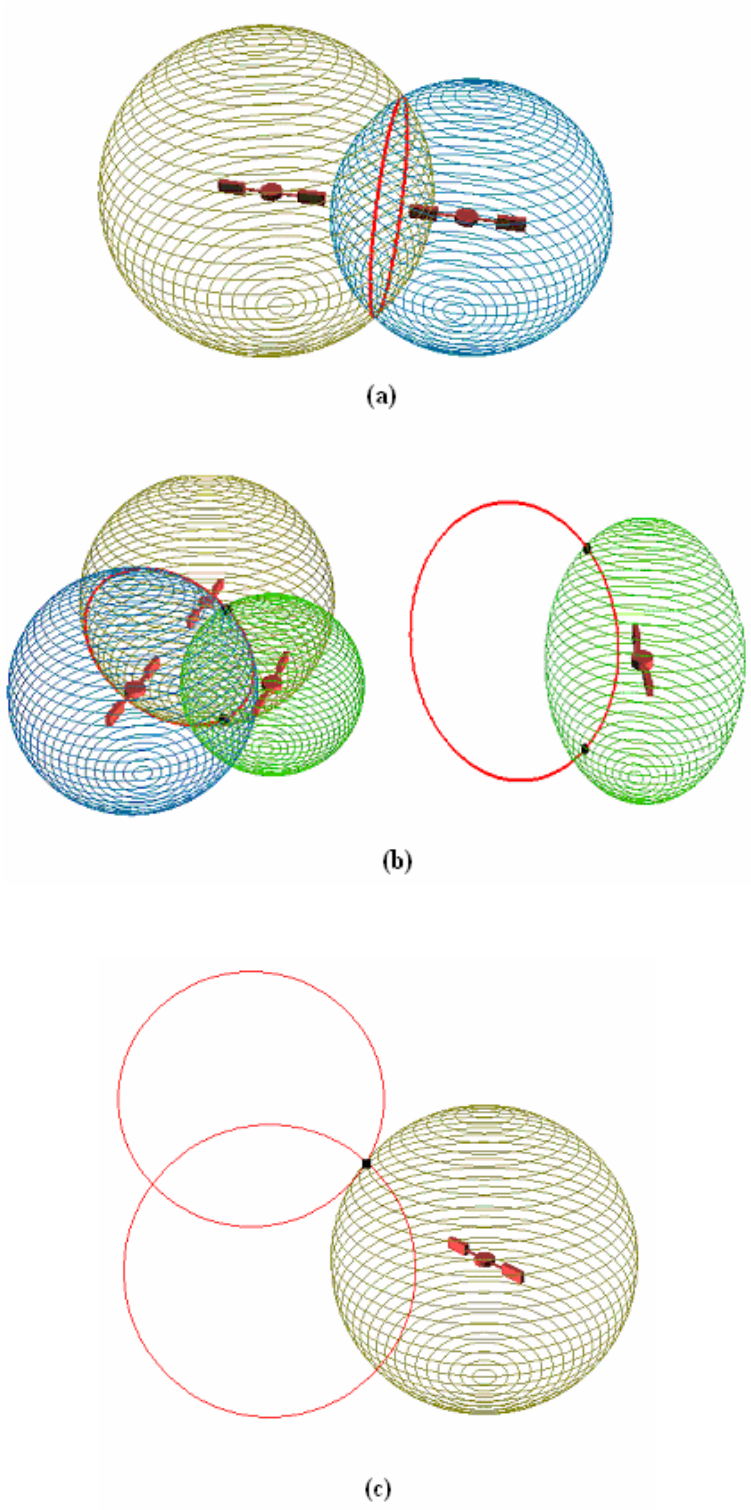


Figure 4.7 Illustration of multilateration technique (a) Intersection of two spheres (b) Intersection of three spheres (c) Intersection of four sphere (Source : WEB_6 2005)

Mathematically the multilateration technique has similar basics with 2D-trilateration. It also uses geometrical principles to find the exact position of the target point. As similar to the 2D-trilateration technique, multilateration gives the exact position of the target point in 3D space in case of known the exact positions of receivers. In this technique the value of distance between target point and the receivers creates a sphere around the receiver. The intersection of the spheres gives the exact position of the target point in 3D space.

Figure 4.7 shows how multilateration works. Each satellite shape figure represents beacons with known locations. From the first beacon's signal, it can be determined that the object should be located at sphere centred at first beacon. Similarly, from second, third and fourth beacon's signals, it can be determined that the object should be located at the spheres centred at second, third and fourth beacons, respectively. Thus, the intersection of the four spheres is the estimated location of the target point.

# CHAPTER 5

# LATERAL INHIBITION SIMULATIONS

## 5.1. Contrast Enhancement Effect

As it was mentioned in Chapter 3, lateral inhibition has three effects. The contrast enhancement effect is one of them. In the light of the observations which had been made on animals such as Horseshoe Crab and human nervous system it is expected that lateral inhibition mechanism exaggerates the discontinuity on the input. To simulate this effect on a sensory system an array contains 19 light dependent resistors were constructed. LDRs were placed abreast and the distances between them were equal. Then the light source was placed 230 mm above the LDRs. The light source was moved horizontally and first 5 LDRs were illuminated from this level then light source were started to move vertically in addition to the horizontal movement. For each measurement the light source was brought near 10 mm to the sensors. Next 8 measurements were taken with this technique. This process created a discontinuity on the input. When the light source was on the 14th LDR the distance between sensors and the light source was 150 mm. Then the remaining 6 LDRs were illuminated from 150 mm.

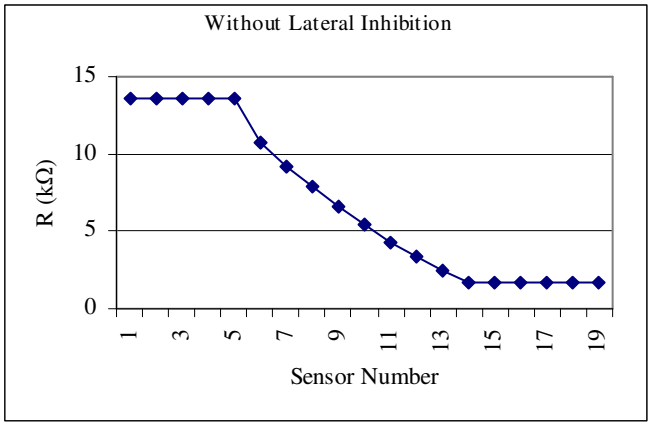


Figure 5.1 Response of LDRs without lateral inhibition

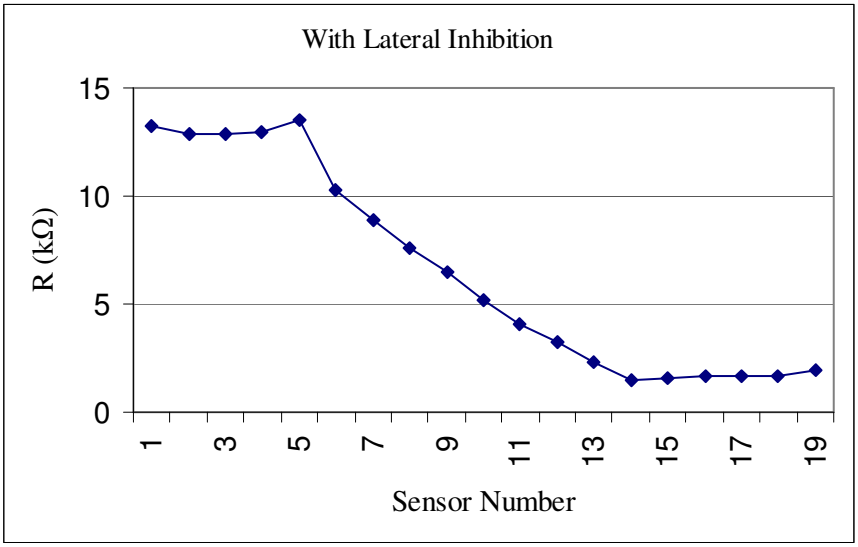


Figure 5.2 Contrast enhancement by lateral inhibition

Figure 5.1 shows the response of each light dependent resistor to the illumination. When the light source get closer to the LDRs the resistance of the LDRs decreases. Figure 5.2 shows the response of LDRs after applying lateral inhibition mechanism. It is clearly seen that the discontinuity which starts with 5th sensor and ends in 14th sensor is exaggerated by the lateral inhibition mechanism. While the distance between 5th LDRs resistance value and 14th LDR resistance value was 11.85kΩ, this difference increased to 12.06 kΩ after applying Lateral Inhibition mechanism.

## 5.2. Funneling Effect

Another effect of lateral inhibition which was simulated on sensory array that consist of LDRs is funnelling effect. To observe the funnelling effect on sensory array 17 LDRs were placed abreast and the distance between the LDRs was equal. The light source was placed 200 mm above the first LDR and it was moved down 10 mm through the LDRs before each measurement up to 9th LDR. When the light source was on the 9th LDR the distance between light source and LDRs was 120 mm. After 9th LDR the light source was moved up 10 mm before each measurement so when the light source was on the 17th LDR the distance between the light source and LDRs was again 200

mm. Figure 5.3 shows the responses of the light dependent resistors under the conditions that described above.

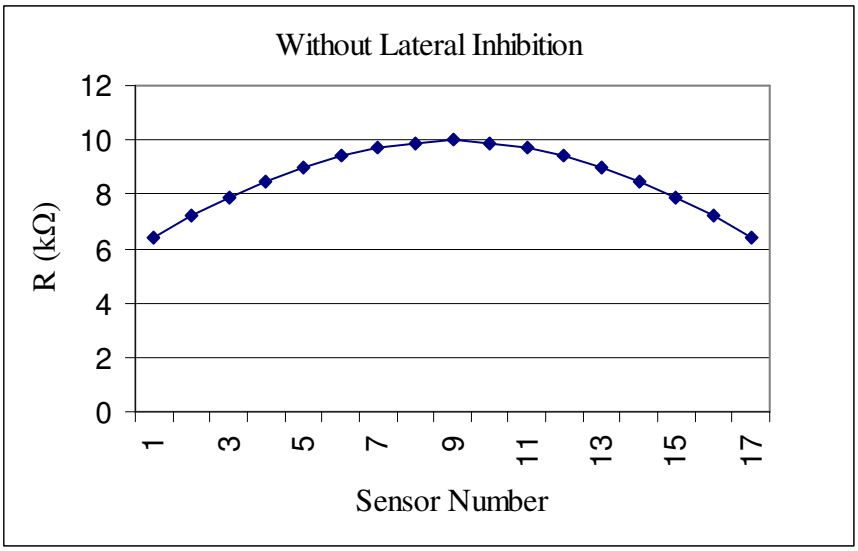


Figure 5.3 Response of LDRs without lateral inhibition

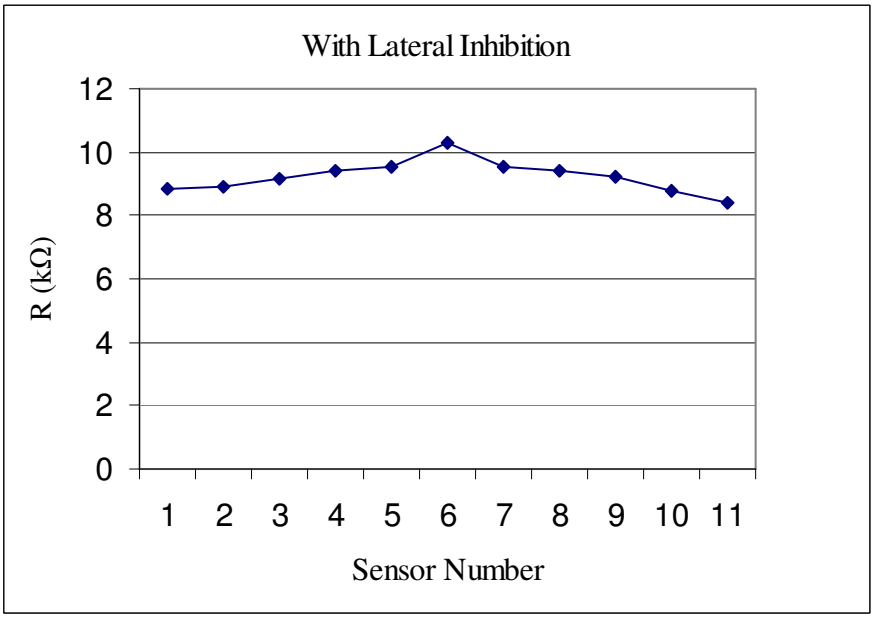


Figure 5.4 Funnelling by lateral inhibition

Figure 5.4 shows the effect of lateral inhibition on the response of LDRs. It is clearly seen that the strongly illuminated LDRs drive down the other ones which are illuminated weaker. As a result of this competition the response of input that applied on a large area get sharpen and it makes the stimulus more distinguishable. In the light of previous observations on human sensory and nervous system it is known that funnelling effect becomes useful after several relay points. Figure 5.4 shows the response of LDRs after six relay points. In Figure 5.5 the changes that occur after each relay points on the LDRs responses can be seen.

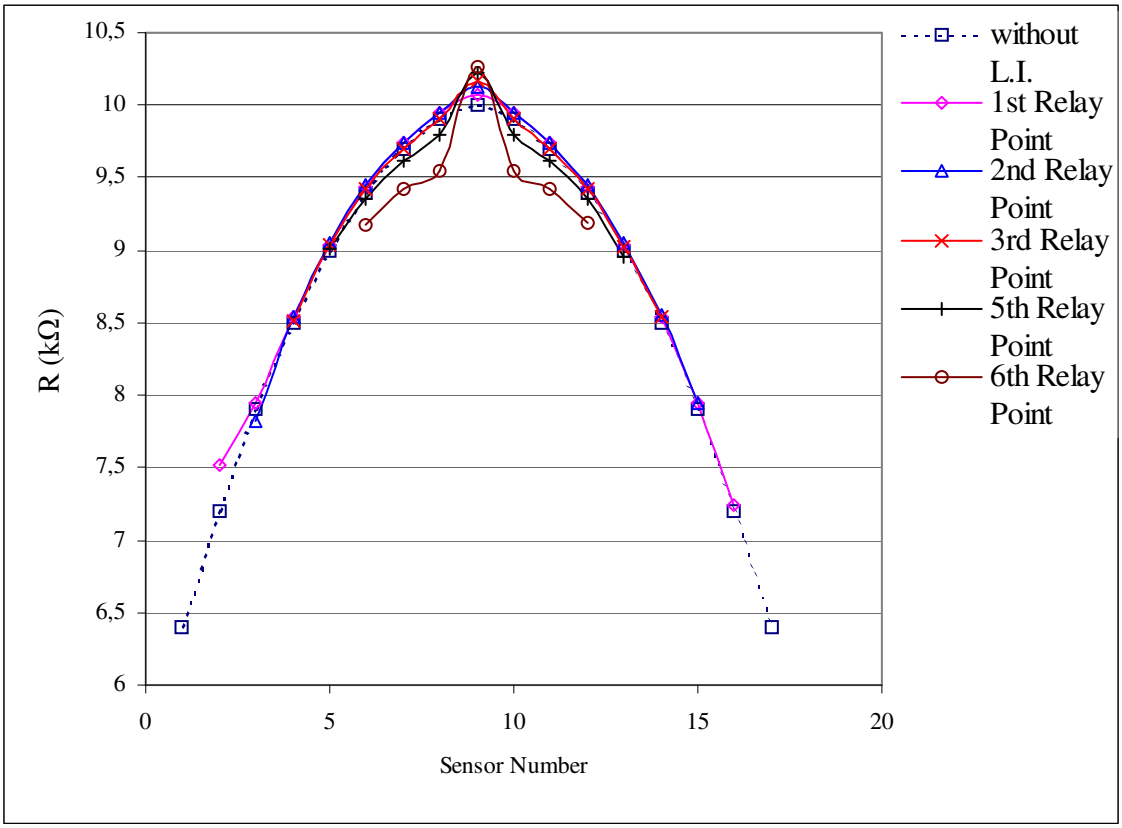


Figure 5.5 Effect of several relay on the funnelling.

## 5.3. Two Point Discrimination Effect

To observe two point discrimination effect, two light sources were implemented which were close to each other. The light sources were not moved during the simulation. To achieve this simulation 13 LDRs were placed abreast and the distances between them were equal. In Fig. 5.6 outputs of the LDRs illuminated by these two

light sources with and without lateral inhibition can be seen. Here the peaks are the points where the input is the strongest. When lateral inhibition mechanism was applied to the responses of LDRs the two peaks which represents the number of light source becomes more distinguishable.

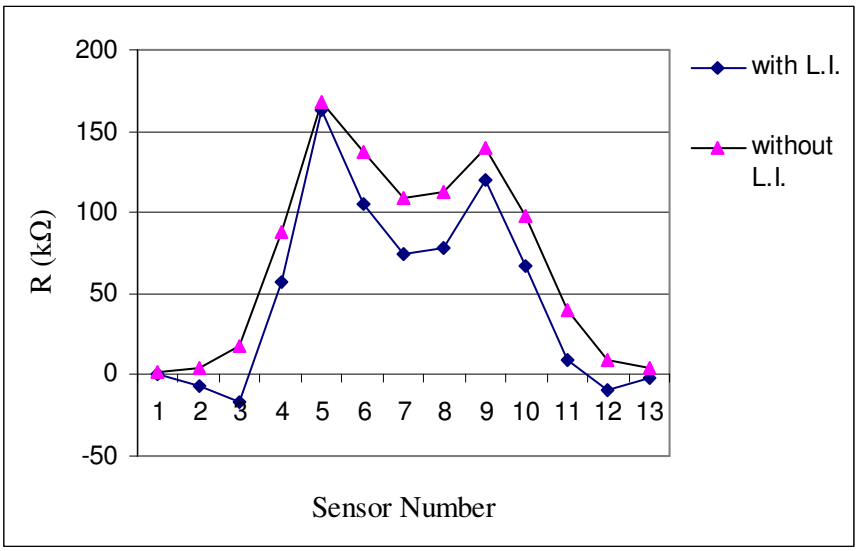


Figure 5.6 Two point discrimination by lateral inhibition

## 5.4. Target Localization

As it was mentioned in earlier sections the lateral inhibition mechanism has important effects on biological sensory networks. To obtain similar effects and to observe the efficiency of lateral inhibition mechanism on the photosensitive sensors (LDR and photodiode) an experimental setup was constructed which is expected to make an target localization as it was described in first part of this chapter.

Firstly, the response of photosensitive sensor to different illumination level which was adjusted by changing the position of the light source was recorded. This process were done by using both type of photosensitive sensor and named as calibration.

### 5.4.1. Calibration Of Light Dependent Resistor (LDR)

Figure 5.7 and figure 5.8 show the response of light dependent sensor depending on the distance between the light source and LDR. When the distance between the light source and LDR increases the resistance of LDR increases. As it is seen in Figure 5.7 and Figure 5.8 a relation between the resistance of LDRs and the distance between the light source is not linear.

In this calibration process two types of LDR were used. The first one has 10 mm diameter which is known as a standard LDR and the second one has 5 mm diameter which is rarely used in circuits. For Ø10 mm LDR the resistance values can be fitted with a curve which given below :

$$R = 0.0082d^2 - 1.6378d + 124.92 \quad (5.1)$$

For Ø5 mm LDR the resistance values can be fitted a curve which equation is given below :

$$R = 0.0013d^2 + 0.0492d + 45.329 \quad (5.2)$$

where 'R' represents the resistance and 'd' represents the distance between LDR and the light source.

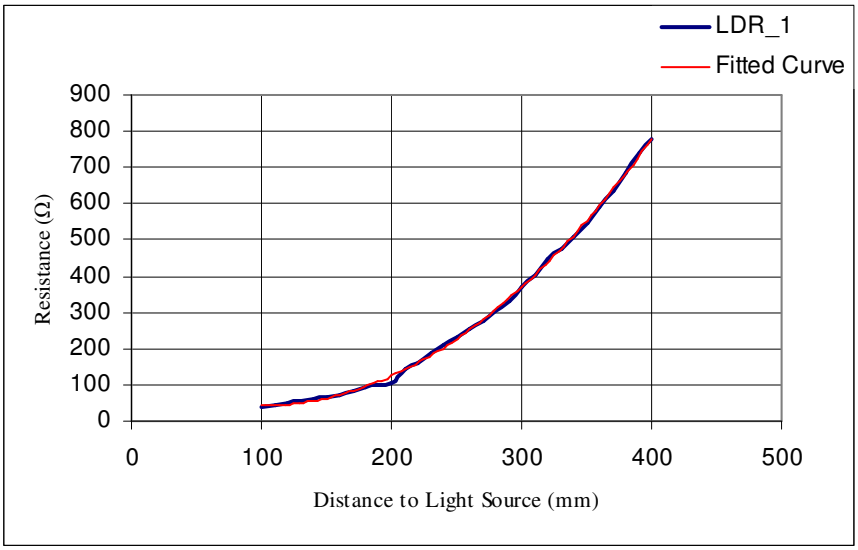


Figure 5.7 Resistance values of Ø10mm LDR

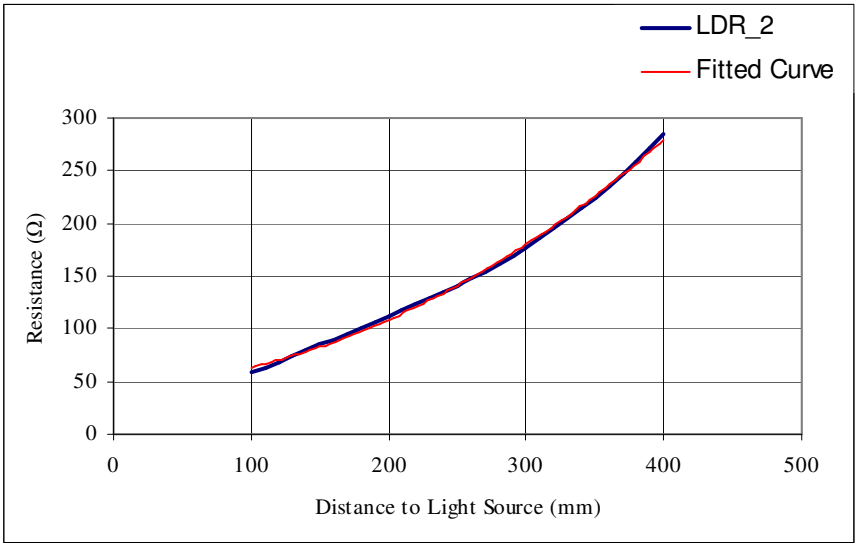


Figure 5.8 Resistance values of Ø5mm LDR

During continual the measurements, although the experimental conditions and the light source which was used to stimulate the LDRs were the same, an inconsistency was observed in the response of the LDRs. It is thought that this inconsistency resulted from the unequal semiconductor pattern which is deposited on the LDRs. In the light of this opinion, it was decided to take all measurement by using the same LDR. But this did not make the measurements consistent.

When this situation analysed in detail it is observed that the resistance values which were taken in the morning were always lower than the resistance values which were taken in the afternoon. It showed that the LDRs resistance was influenced by the previous illumination conditions. This situation is called light history effect.

The light history effect can be clearly seen in Figure 5.9 and Figure 5.10. Both LDRs (Ø10mm and Ø5mm) were stored under dark conditions for 16 hours. Then they were illuminated and the resistance values were recorded. The curves that display these resistance values for each type of LDR are named as DARK in Figure 5.9 and in Figure 5.10. After that the same LDRs were stored under light conditions for 6 hours and they were illuminated by the same light source then their resistance values were recorded. The curves that display these resistance values for each type of LDR are named as LIGHT in Figure 5.9 and Figure 5.10.

It is obvious that light history effect makes the measurements unreliable. Therefore it was decide to use photodiodes instead of light dependent resistors.

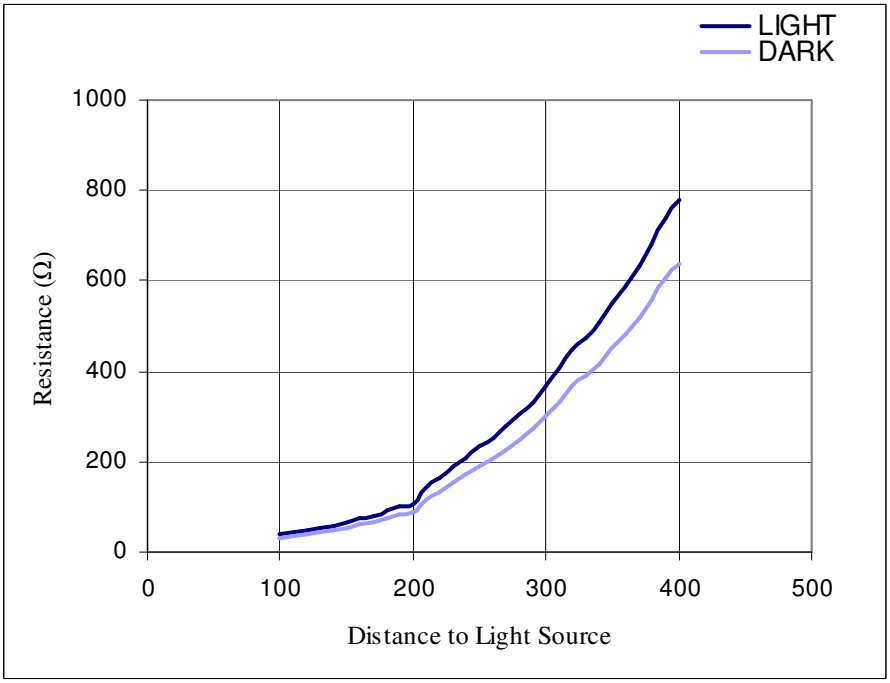


Figure 5.9 Light and dark resistances of Ø10mm LDR

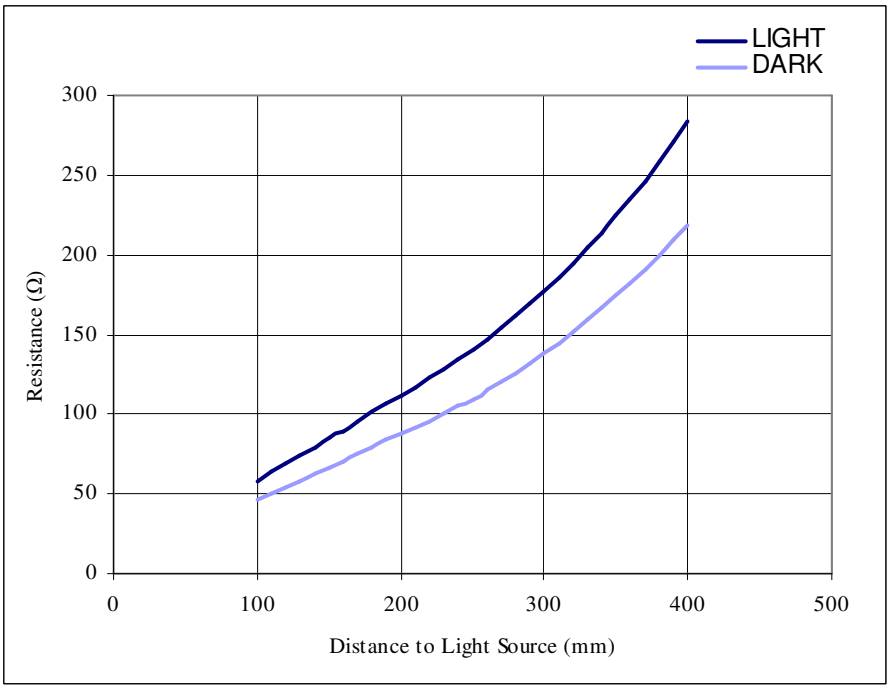


Figure 5.10 Light and dark resistances of Ø5mm LDR

## 5.4.2. Calibration Of Photodiodes

Figure 5.11 and Figure 5.12 show the response of silicon photodiodes depending on the distance between the light source and photodiodes. When the distance between the light source and photodiodes increases the voltage output of the photodiode decreases. As it is seen in Figure 5.11 and 5.12 the relation between the voltage value of photodiodes and the distance between the light source is not linear.

In this calibration process two types of photodiodes were used. The first one has silicon (Si) material as a semiconductor and the second one has germanium (Ge) semiconductor material. For first silicon photodiodes the voltage values were fitted with a curve given below :

$$V = 1.0684*d^{-0.1126} \tag{5.3}$$

For second silicon photodiodes the voltage values can be fitted with a curve given below :

$$V = 1.0605*d^{-0.1104} \tag{5.4}$$

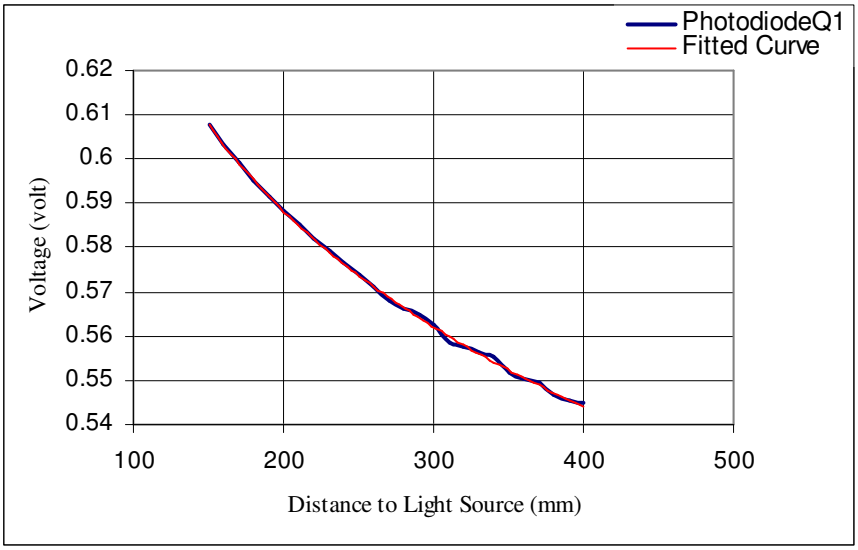


Figure 5.11 Voltage values of first silicon photodiodes

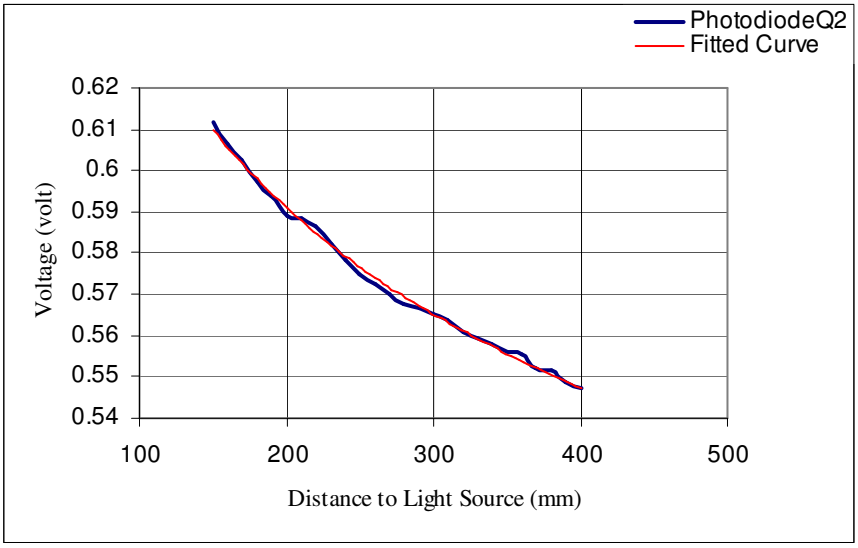


Figure 5.12 Voltage values of second silicon photodiodes

Figure 5.13 and figure 5.14 show the response of germanium photodiodes depending on the distance between the light source and photodiodes. This type of photodiodes has a similar characteristics with the silicon photodiodes. For first germanium photodiodes the voltage values can be fitted with a curve which equation is given below :

$$V = 1.0367*d^{-0.242} \qquad (5.5)$$

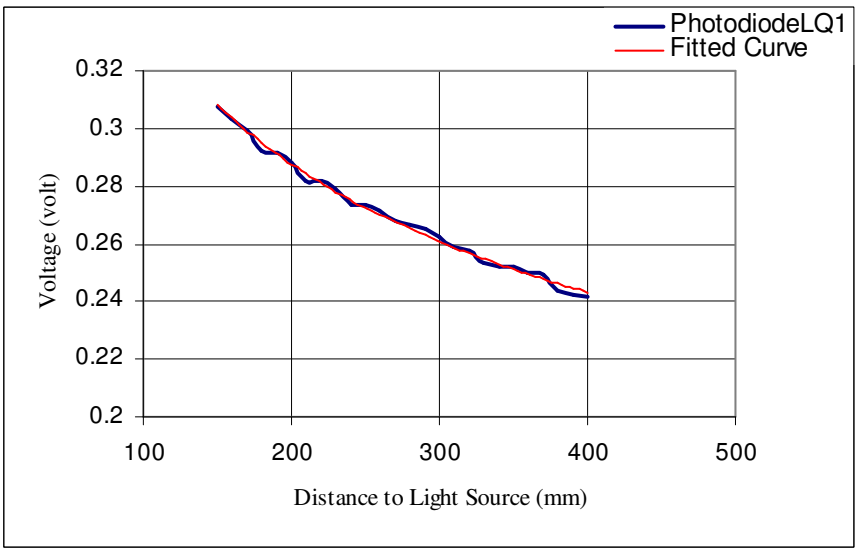


Figure 5.13 Voltage values of first germanium photodiode

For second germanium photodiodes the voltage values can be fitted a curve which equation is given below :

$$V = 0.9765d^{*-0.229} \tag{5.6}$$

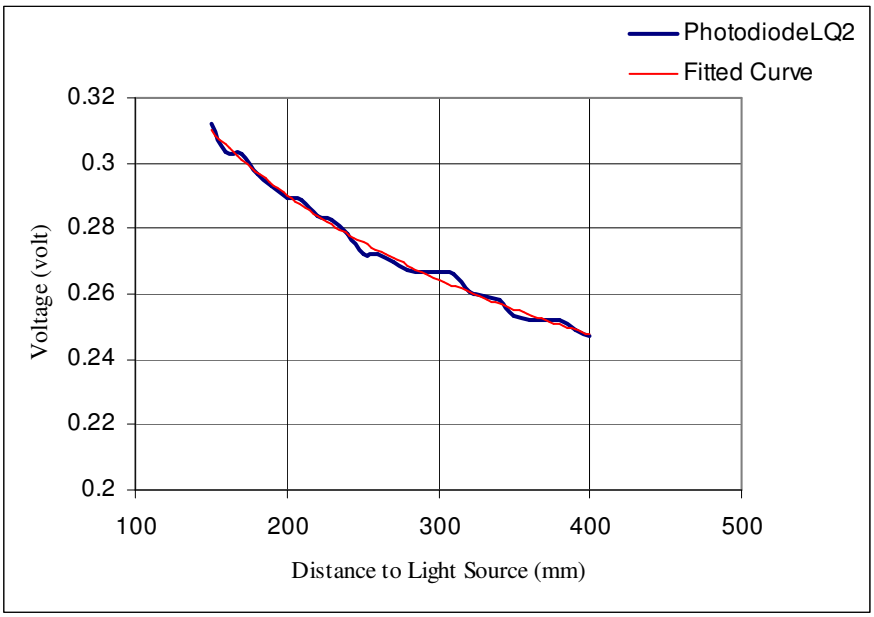


Figure 5.14 Voltage values of second germanium photodiodes

In the Table 5.1, a comparison between light dependent resistor and photodiode characteristics is given. The better sensitivity, linearity and reproducibility characteristics make the photodiodes appropriate sensors for this study.

Table 5.1. Comparison of photodiode and light dependent resistor characteristics.

| Sensor Type | Available Wavelengths (μm) | Performance to-cost ratio | Sensitivity | Linearity | Stability | Reproducibility | Cost | Physical Size |
|---|---|---|---|---|---|---|---|---|
| **light dependent resistor** | 0.4 - 0.7 | Excellent | Very Good | Good | Poor | Poor | Very Low | Small |
| **photo diode** | 0.2 - 2.0 | Good | Very Good | Excellent | Very Good | Excellent | Low | Small |

## 5.4.3. Lateral Inhibition On Localization

After calibration described in Part 5.4.2, several photodiode arrays were constructed to localize the light source which had been adjusted on the experimental setup. These arrays consisted of two different kinds of photodiodes that were relatively high and low quality photodiodes.

In the scope of the experimental process, the voltage values taken from photodiodes were processed according to the calibration and transferred into a distance to the light source. These distances were used to localize the light source. For this localization process the trilateration method and an algorithm ($TbHP^{+}$) which was written in the Matlab© programming language were used. The same process was conducted for each photodiode array by applying lateral inhibition mechanism.

In lateral inhibition process, it is assumed that each photodiode has an interconnection with the three closest neighbour photodiodes. Lateral inhibition process was applied to photodiode array according to the Equation 2.8 which was given in Chapter 2. As an inhibition coefficient (β) 0.05 was chosen and as an excitatory coefficient (α) 0.145 was chosen.

As a first step an array which contains 9 (3x3) high quality photodiodes was constructed . The X coordinate of light source was adjusted as 41 and Y and Z coordinates were adjusted as 45, 200 respectively. The coordinates of photodiodes and the measurement results are tabulated in Table 5.2. The result of localization process

which was done by using high quality photodiode array can be seen in Table 5.3. After localization process, the estimated coordinates and the real coordinates of the light source were compared. The result of this comparison is given in Table 5.5. The result of applying lateral inhibition to localization process which was done for the same photodiode array are also given in Table 5.3. Comparison of the real coordinates and the estimated coordinates of the light source after applying lateral inhibition mechanism are seen in Table 5.5.

Table 5.2. Results of measurement with 9 high quality photodiodes.

| **Photodiode Number** | **Coordinates** | | | **Measured voltage (volt)** | **Estimated total distance (mm)** | **Voltage after L.I. (volt)** | **Estimated total distance after L.I. (mm)** |
|---|---|---|---|---|---|---|---|
| | **X** | **Y** | **Z** | | | | |
| 1 | 0 | 45 | 0 | 0.5903 | 194.46 | 0.5874 | 203.31 |
| 2 | 41 | 45 | 0 | 0.5915 | 191.18 | 0.5887 | 199.35 |
| 3 | 82 | 45 | 0 | 0.5901 | 195.13 | 0.5871 | 204.14 |
| 4 | 0 | 80 | 0 | 0.5892 | 197.96 | 0.5862 | 206.91 |
| 5 | 41 | 80 | 0 | 0.5905 | 194.07 | 0.5877 | 202.48 |
| 6 | 82 | 80 | 0 | 0.5893 | 197.61 | 0.5864 | 206.50 |
| 7 | 0. | 115 | 0 | 0.5863 | 206.85 | 0.5829 | 217.72 |
| 8 | 41 | 115 | 0 | 0.5880 | 201.57 | 0.5850 | 210.66 |
| 9 | 82 | 115 | 0 | 0.5867 | 205.60 | 0.5833 | 216.23 |

Table 5.3. Result comparison of high quality array and low quality array.

| Sensor Type | Real Coordinates | | | TbHP$^{+}$ | | | Trilateration | | |
|---|---|---|---|---|---|---|---|---|---|
| | X | Y | Z | X | Y | Z | X | Y | Z |
| **High quality sensors without L.I.** | 41 | 45 | 200 | 37.79 | 39.21 | 189.01 | 35.93 | 56.74 | 195.19 |
| **High quality sensors with L.I.** | 41 | 45 | 200 | 42.06 | 43.75 | 199.57 | 39.99 | 46.19 | 202.65 |
| **Low quality sensors without L.I.** | 41 | 45 | 200 | 34.04 | 33.62 | 178.1 | 28.14 | 63.51 | 194.09 |
| **Low quality sensors with L.I.** | 41 | 45 | 200 | 43.18 | 42.43 | 188.65 | 29.03 | 58.96 | 198.92 |

Then the localization process was repeated by using an array which contains low quality photodiodes. The number of photodiodes was constant with the previous array. The localization process with low quality photodiodes was done with and without applying lateral inhibition mechanism. The coordinates of photodiodes and the measurement results are listed in Table 5. The results of the localization processes are shown in Table 5.3 and 5.5.

Table 5.4. Results of measurement with 9 low quality photodiodes.

| Photodiode Number | Coordinates | | | Measured voltage (volt) | Estimated total distance (mm) | Voltage after L.I. (volt) | Estimated total distance after L.I. (mm) |
|---|---|---|---|---|---|---|---|
| | X | Y | Z | | | | |
| 1 | 0 | 45 | 0 | 0.29218 | 187.16 | 0.29081 | 190.90 |
| 2 | 41 | 45 | 0 | 0.29281 | 185.48 | 0.29148 | 189.06 |
| 3 | 82 | 45 | 0 | 0.29177 | 188.27 | 0.29034 | 192.21 |
| 4 | 0 | 80 | 0 | 0.29018 | 192.64 | 0.28872 | 196.75 |
| 5 | 41 | 80 | 0 | 0.29178 | 188.24 | 0.29051 | 191.71 |
| 6 | 82 | 80 | 0 | 0.29022 | 192.53 | 0.28878 | 196.60 |
| 7 | 0 | 115 | 0 | 0.28666 | 202.77 | 0.28470 | 208.69 |
| 8 | 41 | 115 | 0 | 0.28852 | 197.34 | 0.28708 | 201.51 |
| 9 | 82 | 115 | 0 | 0.28696 | 201.88 | 0.28504 | 207.65 |

Table 5.5. Error comparison of high quality array and low quality array.

| Sensor Type | Error % | | | | | |
|---|---|---|---|---|---|---|
| | $TbhP^+$ | | | Trilateration | | |
| | X | Y | Z | X | Y | Z |
| **High quality sensors without L.I.** | 7.83 | 12.85 | 5.49 | 12.37 | 26.08 | 2.40 |
| **High quality sensors with L.I.** | 2.58 | 2.79 | 0.21 | 2.46 | 2.64 | 1.33 |
| **Low quality sensors without L.I.** | 16.98 | 25.29 | 10.95 | 31.37 | 41.13 | 2.96 |
| **Low quality sensors with L.I.** | 5.32 | 5.71 | 5.68 | 29.20 | 31.02 | 0.54 |

To observe the effects of the sensor number on the localization an array which contained 16 (4 x 4) low quality photodiodes was constructed. At first the coordination of the light source was localized without applying lateral inhibition. Then the localization process was repeated with lateral inhibition mechanism. The coordinates of photodiodes and the measurement results are listed in Table 5.6. The results of the localization processes are shown in Table 5.7 and 5.8.

Table 5.6. Results of measurement with 16 low quality photodiodes.

| Photodiode Number | Coordinates | | | Measured Voltage (volt) | Estimated total distance (mm) | Voltage after L.I (volt) | Estimated total distance after L.I. (mm) |
|---|---|---|---|---|---|---|---|
| | X | Y | Z | | | | |
| 1 | 0 | 45 | 0 | 0.29319 | 184.46 | 0.29164 | 188.62 |
| 2 | 27.3 | 45 | 0 | 0.29480 | 180.28 | 0.29342 | 183.86 |
| 3 | 54.6 | 45 | 0 | 0.29544 | 178.64 | 0.29418 | 181.87 |
| 4 | 82 | 45 | 0 | 0.29319 | 184.46 | 0.29160 | 188.74 |
| 5 | 0 | 68.3 | 0 | 0.29275 | 185.63 | 0.29138 | 189.33 |
| 6 | 27.3 | 68.3 | 0 | 0.29378 | 182.92 | 0.29233 | 186.75 |
| 7 | 54.6 | 68.3 | 0 | 0.29398 | 182.39 | 0.29257 | 186.11 |
| 8 | 82 | 68.3 | 0 | 0.29275 | 185.63 | 0.29137 | 189.36 |
| 9 | 0 | 91.6 | 0 | 0.28947 | 194.64 | 0.28789 | 199.15 |
| 10 | 27.3 | 91.6 | 0 | 0.29214 | 187.26 | 0.29080 | 190.93 |
| 11 | 54.6 | 91.6 | 0 | 0.29254 | 186.19 | 0.29139 | 189.31 |
| 12 | 82 | 91.6 | 0 | 0.28947 | 194.64 | 0.28787 | 199.20 |
| 13 | 0 | 114.9 | 0 | 0.28604 | 204.62 | 0.28404 | 210.73 |
| 14 | 27.3 | 114.9 | 0 | 0.28784 | 199.31 | 0.28626 | 203.95 |
| 15 | 54.6 | 114.9 | 0 | 0.28804 | 198.72 | 0.28648 | 203.29 |
| 16 | 82 | 114.9 | 0 | 0.28604 | 204.62 | 0.28401 | 210.82 |

Table 5.7. Result comparison of 9 high quality photodiodes and 16 low quality photodiodes.

| Sensor Type | Real Coordinates | | | $TbHP^+$ | | | Trilateration | | |
|---|---|---|---|---|---|---|---|---|---|
| | X | Y | Z | X | Y | Z | X | Y | Z |
| **9 High quality sensors without L.I.** | 41 | 45 | 200 | 37.79 | 39.21 | 189.01 | 35.93 | 56.74 | 195.19 |
| **16 Low quality sensors without L.I.** | 41 | 45 | 200 | 34.06 | 36.55 | 180.15 | 52.33 | 32.10 | 184.75 |
| **16 Low quality sensors with L.I.** | 41 | 45 | 200 | 45.83 | 45.69 | 186.76 | 46.78 | 43.05 | 195.04 |

Table 5.8. Error comparison of 9 high quality photodiodes and 16 low quality photodiodes.

| Sensor Type | Error % | | | | | |
|---|---|---|---|---|---|---|
| | $TbhP^+$ | | | Trilateration | | |
| | X | Y | Z | X | Y | Z |
| **9 High quality sensors without L.I.** | 7.83 | 12.85 | 5.49 | 12.37 | 26.09 | 2.41 |
| **16 Low quality sensors without L.I.** | 16.93 | 18.78 | 9.92 | 27.63 | 28.67 | 7.63 |
| **16 Low quality sensors with L.I.** | 11.77 | 1.53 | 6.62 | 14.10 | 4.33 | 2.48 |

It is clearly seen in Table 5.3 and Table 5.7 that by lateral inhibition, estimates converge to the real coordinates. Although the same number of and same quality photodiodes were used for both measurements, the deviation in the localization of the position of the light source decreased. It proves that lateral inhibition mechanism provides more sensitive localization. In addition, applying lateral inhibition to sensory arrays with high in number and low in quality photodiodes provides localization as sensitive as the array which contains less number of high quality photodiodes. It is clearly seen in Table 5.5. that in the case of using low quality array the error value for X axis 11.77 % and Z axis 6.62 % is kept close to the error value 7.84 % for X axis and

5.49 % for Z axis which was obtained by using high quality sensory array without lateral inhibition mechanism. Similarly for Y axis low quality sensory array gives better result 1.53 % than high quality sensory array as a result of lateral inhibition mechanism.

# CHAPTER 6

# CONCLUSION

In this study, Lateral Inhibition mechanism which is also known as contrast enhancement mechanism by biologists, was examined. Lateral inhibition is a basic data processing principle for biological systems and it is commonplace for biological DSNs including human sensory and nervous systems. The interactions within L.I. can be excitatory or inhibitory. As a result of lateral inhibition mechanism, each sensor drives down the neighbour sensors in proportion to its own value. It has an important role for human vision, audition and somatic sensation. Although the lateral inhibition mechanism has a different contribution at the different level of all sensory pathways, there is one major effect for each sensory system. These effects were classified in three groups:

i. contrast enhancement effect for vision

ii. funnelling effect for audition

iii. two – point discrimination effect for somatic sensation

An experimental set up for getting the effects of lateral inhibition was built up. It consisted of photosensitive sensors and adjustable light source. It was observed that, the same effects of lateral inhibition which play important role for biological systems are operative for photosensitive sensors. Each photosensitive sensor was calibrated relative to the distance to the light source. The output of each sensor was converted into a distance value and this value was employed to localize the position of the light source. Localization process was done by using trilateration method and an algorithm called " $TbHP^{+}$ " written in the Matlab© programming language. Lateral inhibition was applied to the data from the setup. Results showed that lateral inhibition mechanism increased the sensitivity of localization. When the estimated coordinates and the real coordinates of the light source were compared it was observed that the lateral inhibition for identical sensory network which contains 9 (3 x 3) high quality sensors reduced error values from 7.83 %, 12.85 %, 5.49 % to 2.58 %, 2.79 % , 0.21% for X , Y and Z axises respectively. The localization process was repeated by using another network that contains 16 ( 4 x 4) low quality and low cost sensors. It was seen that the result of localization process done by low quality sensors with lateral inhibition converged to the

result which were taken by using high quality sensory network without lateral inhibition. The error values for low quality sensory array decreased from 16.93 %, 18.78 %, 9.92 % to 11.77 %, 1.53, 6.62 % for X, Y and Z axises respectively. For high quality sensory network the error values were calculated as 7.83 %, 12.85 %, 5.49 % for X , Y and Z axises respectively.

Lateral inhibition has a great application potential for the artificial intelligence field. The competition among sensors has benefits. The reduction of redundancy is one of the most important advantages of lateral inhibition. For some sensory systems lateral inhibition acts as a low-pass filter. To apply L.I. rules the most important study will be the determination and optimization of the strength of inhibition (β) and self-excitation (α) values.

# REFERENCES


Abramov, I., Bernhard, C.G., Hartline, H.K., Ratliff, F., Tomita, T., 1972. 'Physiology of Photoreceptor Organs' edited by Fuortes, M.G.F., (Springer-Verlag, New York) pp. 381-414

Barlow, H.B. 1982 ' The Senses'. edited by Mollon J.D. (Cambridge University Press), pp. 307-331

Barlow, R.B., 1969. 'Inhibitory Fields in the Limulus Lateral Eye' *Journal of General Physiology*, Vol. 54 pp. 383-397

Barlow, R.B., Fraioli, A.J. 1978. 'Inhibition in the *Limulus* Lateral Eye' *The Journal Of General Physıology*. Vol.71, pp. 699-721

Barlow, R.B., Hitt, J.M., Dodge, F.A. 2000. 'Limulus Vision in the Marine Environment' Invertebrate Sensory Information Processing: Implications for Biologically Inspired Autonomous Systems Workshop, Massachussets, (15-17 April 2000)

Barlow, R.B., Kaplan, E. 1975. 'Properties of Visual Cells in the Lateral Eye of Limulus *Extracellular Recordings*' *Journal of General Physiology*, Vol. 66, pp.. 303-326

Barlow, R.B., Kaplan, E. 1977. 'Properties of Visual Cells in the Lateral Eye of Limulus *Intracellular Recordings*' *Journal of General Physiology*, Vol. 69, pp. 203-220

Barlow, R.B., Kaplan, E., Renninger, G.H., Saito, T. 1987. 'Circadian Rhythms in Limulus Photoreceptor' *Journal of General Physiology*, Vol 89, pp. 353-387

Barlow, R.B., Prakash, R., Solessio, E. 1993. 'The Neural Network of the Limulus Retina: From Computer to Behaviour'. *American Zoologist*, Vol. 33, pp. 66-78

Barlow, R.B., Quarles, D.A. 1975. 'Mach Bands in the Lateral Eye of Limulus' *Journal of General Physiology*, Vol. 65, pp. 709-730

Bicchi, A. 2000. 'Hands for Dexterous Manipulation and Robust Grasping: A Difficult Road Toward Simplicity'. *IEEE Transactıons On Robotıcs And Automatıon*, Vol. 16, No. 6

Bicchi, A., Salisbury, J.K. and Brock, D.L. "Contact Sensing from Force Measurements'. 2000. *Massachusetts Institute of Technology Artificial Intelligence Laboratory.*

Brodie, S.E., Knight, B.W., Ratliff, F. 1978. 'The Spatiotemporal Transfer Function of the Limulus Lateral Eye' *Journal of General Physiology*, Vol. 72, pp. 167-202

Brooks, M., 1988 'Highly Redundant Sensing in Robotics -Analogies From Biology: Distributed Sensing and Learning'. *NATO Advanced Research Workshop on Highly Redundant Sensing in Robotic Systems*, Italy.

Davison, A., Feng, J., Brown, D. 1999. 'Structure of lateral inhibition in an olfactory bulb model'. *Laboratory of Computational Neuroscience, The Babraham Institute.*

Dynamics of Excitation and Inhibition in the Eye of Limulus'. *The Journal Of General Physıology*. Vol. 56.

Egger, V. Svoboda, K. and Mainen, Z.F., 2003. 'Mechanisms of Lateral Inhibition in the Olfactory Bulb: Efficiency and Modulation of Spike-Evoked Calcium Influx into Granule Cells'. The Journal of Neuroscience, Vol. 23, pp. 7551-7558.

Hancock, K.E., Davis K.A., Voigt, H.F. 1997. 'Modeling inhibition of type II units in the dorsal cochlear nucleus' . *Biol. Cybern.* Vol.76, pp. 419-428

Hartline, H.K., Ratliff, F. 1958. 'Spatıal Summatıon Of Inhıbıtory Influences In The Eye Of Lımulus, And The Mutual Interactıon Of Receptor Unıts' *Journal of General Physiology*, Vol. 41, No 5

Hartline, H.K., Wagner, H.G., Ratliff, F. 1955. 'Inhıbıtıon In The Eye Of Lımulus' *The Journal of General Physiology*, Vol.39, No 5

Hudspeth, A. J., 1997. 'Mechanical amplification of stimuli by hair cells'. *Current Opinion in Neurobiology ,*Vol. 7, pp. 480-486

Husain, F.T., Tagamets, M.A., Fromm, S.J., Braun, A.R., Horwitz, B. 2004. 'Relating neuronal dynamics for auditory object processing to neuroimaging activity: a computational modeling and an fMRI study'. *NeuroImage*, Vol.21, pp. 1701-1720

Jackler, R.K., Blevins N.H. "Exposure of the lateral extremity of the internal auditory canal through the retrosigmoid app.roach: a radioanatomic study." *Otolaryngol Head Neck Surg.* 1994; Vol.111: 1, pp. 81-90.

Kaplan, E., Barlow, R.B., Renninger, G., Purpura, K. 1990. 'Circadian Rhythms in *Limulus* Photoreceptors' *The Journal Of General Physıology*, Vol. 96, pp. 665-685

Knight, B.W., Toyoda, J., Dodge, F.A., 1970. 'A Quantitative Description of the Limulus Photoreceptors' *The Journal of General Physiology*, Vol. 89, pp. 353-378

Lifton, J., Broxton, M., Paradiso, J.A. 'Distributed Sensor Networks as Sensate Skin'. 2003. *Responsive Environments Group – MIT Media Lab.*

Lledo, PM., Gheusi, G. and Vincent, JD. 2005. 'Information Processing in the Mammalian Olfactory System'. *Physiol Rev.,* Vol. 85, pp. 281-317.

Loomis, J.M., 1981. 'Tactile Pattern Perception'. *Perception*, Vol. 10, pp. 5-27

Lowe, M., King, A., Lovett, E. and Papakostas, T. 2004. 'Flexible tactile sensor technology: bringing haptics to life'. *Sensor Review* Volume 24, Number 1, pp.. 33–36

Ma, X. and Suga, N. 2004. 'Lateral Inhibition for Center-Surround Reorganization of the Frequency Map of Bat Auditory Cortex'. *J Neurophysiol* Vol.92, pp. 3192-3199

Meiss, R.A., 1999. 'Medical Physiology' edited by Rhoades, R.A. (Blackwell Press), pp. 63-90

Moore, B.C.J., 1997. 'An Introduction to the Physiology of Hearing' (Academic Press, San Diego) pp. 251-285

Murphy, A.Z., 2002 'Somatosensory System' *Lecture Notes Department of Biology Georgia State University*

Narayan, S.S., Temchin, A.N., Recio, A., Ruggero, M.A., 1984 'Frequency tuning of basilar membrane and auditory nerve fibers in the same cochleae' *Science AAAS,* Vol.282, pp. 1882-1884

Paradiso, J.A., Lifton, J., Broxton M. 2004. 'Sensate Media-multimodal electronic skins as dense sensor networks' *BT Technology* Vol.22 No.4

Pare, M., 2003. 'Sensory Physiology' *Lecture Notes PHGY 210 Queen's University*

Passaglia**,** C.L**.,** Dodge**,** F.A. and Barlow, R.B., 1998., 'Cell Based Model of the Limulus Lateral Eye'. *Journal of Neurophysiology*, Vol.80, pp. 1800-1815

Passaglia, C.L., Dodge, F.A., Barlow, R.B. 1998. 'Cell Based Model of the Limulus Lateral Eye' *Journal of Neuroscience*, Vol. 80, pp. 1800-1815

Plack, C.J., 2004. 'Auditory Perception' (Psychology Press Ltd.) pp. 234-254

Sinclair, I.R., 2001. 'Sensors and Transducers' (Buutterworth-Heinemann ) pp. 53-87

Stiehl W.D. and Breazeal C. 'Affective Touch for Robotic Companions'. 2005. *Robotic Life Group, MIT Media Lab*

Stiehl W.D., 2003. 'Tactile Perception in Robots: From the Somatic Alphabet to the Realization of a Fully Sensitive Skin' . *Bachelor of Science at the Massachusetts Institute of Technology.*

Stiehl, W. D., Lalla, L. and Breazeal, C. 2004. 'A "Somatic Alphabet" App.roach to "Sensitive Skin" ', *Robotic Life Group*.

Urban, N.N., 2002. 'Lateral inhibition in the olfactory bulb and in olfaction' *Physiology & Behavior.,* Vol. 77, pp. 607-612.

Vatesnik, A., Majernik, V., 1998. 'An Algebraic App.roach To The Lateral Inhibition Neural Network' *Department of Theoretical Physics, Faculty of Science, Palacký University.*

Venema, S.C. and Hannaford, B. 1999.' Experıments In Fıngertıp Perceptıon Of Surface Dıscontınuıtıes'. *Biorobotics Laboratory Department of Electrical Engineering University of Washington.*

WEB_1, 2005. University of Daleware Website, 12/04/2005. http://www.udel.edu

WEB_2, 2005. University of Auckland Website, 08/05/2005. http://www.stat.auckland.ac.nz

WEB_3, 2005. Hyperphysics Website, 18/03/2005. http://hyperphysics.phy-astr.gsu.edu/hbase/sound/place.html

WEB_4, 2005. University of Illinois Website, 03/05/2005. http://soma.npa.uiuc.edu

WEB_5, 2005. Perkin Elmer Website, 16/05/2005. www.optoelectronics.perkinelmer.com

WEB_6, 2005. University of Washington Website, 31/05/2005. http://gis.washington.edu/cfr250/lessons/gps

Xie, X., Hahnloser, H.R.R., Seung, S.H. 2002. 'Selectively grouping neurons in recurrent networks of lateral inhibition' *Neural Computation Vol. 14*,pp. 2627-2646.

# APPENDIX A

## $TbHP^{+}$

```
tic
clear


for loop=1:10;

devam=1;
while devam==1;
xin(1,1)=rand; %initial value for x1
xin(2,1)=rand; %initial value for x2
xin(3,1)=rand;
ymax=10000; %initial value for ymax
a=0; %the fittest individual marker
x1arti=0;
x1eksi=0;
x2arti=0;
x2eksi=0;
x3arti=0;
x3eksi=0;
bolum1=1;
bolum2=0;
cx1=0;
cx2=0;
cx3=0;
s=0;
f=0;
p=1; %aging number
ind(1,1)=10;ind(1,2)=5;ind(1,3)=2; %erratic
ind(2,1)=10;ind(2,2)=5;ind(2,3)=3; %fickle
```

```
ind(3,1)=40;ind(3,2)=30;ind(3,3)=5; %greedy
ind(4,1)=20;ind(4,2)=10;ind(4,3)=5; %curious
ind(5,1)=10;ind(5,2)=20;ind(5,3)=25; %normal
ind(6,1)=10;ind(6,2)=30;ind(6,3)=60; %conservative
indmax=90;indmin=2;
errmin(1)=100; errmin(2)=50; errmin(3)=25;
errmax(1)=1000; errmax(2)=500; errmax(3)=100;
fckmin(1)=30; fckmin(2)=20; fckmin(3)=15;
fckmax(1)=100; fckmax(2)=50; fckmax(3)=25;
grdmin(1)=20; grdmin(2)=15; grdmin(3)=10;
grdmax(1)=30; grdmax(2)=20; grdmax(3)=15;
crsmin(1)=10; crsmin(2)=7; crsmin(3)=5;
crsmax(1)=20; crsmax(2)=15; crsmax(3)=10;
normin(1)=2; normin(2)=1; normin(3)=0.5;
normax(1)=10; normax(2)=7; normax(3)=5;
conmax(1)=2; conmax(2)=1; conmax(3)=0.5;
for k=1:1000; %k=iteration number
if bolum1==1;
for i=1:ind(1,p); %i=erratic individuals
   c=rand(1);
   if c>0.5;c=-1;
   else c=1;
   end
   x(1,i)=xin(1,1)+c*xin(1,1)*(errmin(p)+rand(1)*(errmax(p)-errmin(p)))/100;
   x(2,i)=xin(2,1)+c*xin(2,1)*(errmin(p)+rand(1)*(errmax(p)-errmin(p)))/100;
   x(3,i)=xin(3,1)+c*xin(3,1)*(errmin(p)+rand(1)*(errmax(p)-errmin(p)))/100;
end
for i=(ind(1,p)+1):(ind(1,p)+ind(2,p)); %i=fickle individuals
   c=rand(1);
   if c>0.5;c=-1;
   else c=1;
   end
   x(1,i)=xin(1,1)+c*xin(1,1)*(fckmin(p)+rand(1)*(fckmax(p)-fckmin(p)))/100;
   x(2,i)=xin(2,1)+c*xin(2,1)*(fckmin(p)+rand(1)*(fckmax(p)-fckmin(p)))/100;
```

```
    x(3,i)=xin(3,1)+c*xin(3,1)*(fckmin(p)+rand(1)*(fckmax(p)-fckmin(p)))/100;
end
for i=(ind(1,p)+ind(2,p)+1):(ind(1,p)+ind(2,p)+ind(3,p)); %i=greedy individuals
    c=rand(1);
    if c>0.5;c=-1;
    else c=1;
    end
    x(1,i)=xin(1,1)+c*xin(1,1)*(grdmin(p)+rand(1)*(grdmax(p)-grdmin(p)))/100;
    x(2,i)=xin(2,1)+c*xin(2,1)*(grdmin(p)+rand(1)*(grdmax(p)-grdmin(p)))/100;
    x(3,i)=xin(3,1)+c*xin(3,1)*(grdmin(p)+rand(1)*(grdmax(p)-grdmin(p)))/100;
end
for i=(ind(1,p)+ind(2,p)+ind(3,p)+1):(ind(1,p)+ind(2,p)+ind(3,p)+ind(4,p)); %i=curious
individuals
    c=rand(1);
    if c>0.5;c=-1;
    else c=1;
    end
    x(1,i)=xin(1,1)+c*xin(1,1)*(crsmin(p)+rand(1)*(crsmax(p)-crsmin(p)))/100;
    x(2,i)=xin(2,1)+c*xin(2,1)*(crsmin(p)+rand(1)*(crsmax(p)-crsmin(p)))/100;
    x(3,i)=xin(3,1)+c*xin(3,1)*(crsmin(p)+rand(1)*(crsmax(p)-crsmin(p)))/100;
end
for
i=(ind(1,p)+ind(2,p)+ind(3,p)+ind(4,p)+1):(ind(1,p)+ind(2,p)+ind(3,p)+ind(4,p)+ind(5,
p)); %i=normal individuals
    c=rand(1);
    if c>0.5;c=-1;
    else c=1;
    end
    x(1,i)=xin(1,1)+c*xin(1,1)*(normin(p)+rand(1)*(normax(p)-normin(p)))/100;
    x(2,i)=xin(2,1)+c*xin(2,1)*(normin(p)+rand(1)*(normax(p)-normin(p)))/100;
    x(3,i)=xin(3,1)+c*xin(3,1)*(normin(p)+rand(1)*(normax(p)-normin(p)))/100;
end
```

```
for
i=(ind(1,p)+ind(2,p)+ind(3,p)+ind(4,p)+ind(5,p)+1):(ind(1,p)+ind(2,p)+ind(3,p)+ind(4,
p)+ind(5,p)+ind(6,p)); %i=conservative individuals
   c=rand(1);
   if c>0.5;c=-1;
   else c=1;
   end
   x(1,i)=xin(1,1)+c*xin(1,1)*rand(1)*conmax(p)/100;
   x(2,i)=xin(2,1)+c*xin(2,1)*rand(1)*conmax(p)/100;
   x(3,i)=xin(3,1)+c*xin(3,1)*rand(1)*conmax(p)/100;
end

a=0;
for i=1:(ind(1,p)+ind(2,p)+ind(3,p)+ind(4,p)+ind(5,p)+ind(6,p));
   y(i)=9*x(1,i)^2+9*x(2,i)^2+9*x(3,i)^2-1359.42*x(1,i)+182.88*x(2,i)-279011.2909;
   if y(i)<ymax;
      a=i; %fittest individuals, a=i'th individual
   end
end



if a>0;
   if x(1,a)>xin(1,1);
   x1arti=x1arti+1;x1eksi=0;
   elseif x(1,a)<xin(1,1);
   x1eksi=x1eksi+1;x1arti=0;
   end
   if x(2,a)>xin(2,1);
   x2arti=x2arti+1;x2eksi=0;
   elseif x(2,a)<xin(2,1);
   x2eksi=x2eksi+1;x2arti=0;
   end
   if x(3,a)>xin(3,1);
   x3arti=x3arti+1;x3eksi=0;
```

```
elseif x(3,a)<xin(3,1);
x3eksi=x3eksi+1;x3arti=0;
end

sayac=0;
if x1arti>=10;
   cx1=1;
   sayac=sayac+1;
elseif x1eksi>=10;
   cx1=-1;
   sayac=sayac+1;
end
if x2arti>=10;
   cx2=1;
   sayac=sayac+1;
elseif x2eksi>=10;
   cx2=-1;
   sayac=sayac+1;
end
if x3arti>=10;
   cx3=1;
   sayac=sayac+1;
elseif x3eksi>=10;
   cx3=-1;
   sayac=sayac+1;
end
if sayac==3;
   bolum2=1;bolum1=0;
end

ymax=y(a);
xin(1,1)=x(1,a);
xin(2,1)=x(2,a);
xin(3,1)=x(3,a);
```

```
end
elseif bolum2==1; %bolum1 end
for i=1:(floor(ind(1,p)/2)); %i=erratic individuals
   x(1,i)=xin(1,1)+cx1*xin(1,1)*(errmin(p)+rand(1)*(errmax(p)-errmin(p)))/100;
   x(2,i)=xin(2,1)+cx2*xin(2,1)*(errmin(p)+rand(1)*(errmax(p)-errmin(p)))/100;
   x(3,i)=xin(3,1)+cx3*xin(3,1)*(errmin(p)+rand(1)*(errmax(p)-errmin(p)))/100;
end
for i=((floor(ind(1,p)/2))+1):(floor((ind(1,p)+ind(2,p))/2)); %i=fickle individuals
   x(1,i)=xin(1,1)+cx1*xin(1,1)*(fckmin(p)+rand(1)*(fckmax(p)-fckmin(p)))/100;
   x(2,i)=xin(2,1)+cx2*xin(2,1)*(fckmin(p)+rand(1)*(fckmax(p)-fckmin(p)))/100;
   x(3,i)=xin(3,1)+cx3*xin(3,1)*(fckmin(p)+rand(1)*(fckmax(p)-fckmin(p)))/100;
end
for i=((floor((ind(1,p)+ind(2,p))/2))+1):(floor((ind(1,p)+ind(2,p)+ind(3,p))/2));
%i=greedy individuals
   x(1,i)=xin(1,1)+cx1*xin(1,1)*(grdmin(p)+rand(1)*(grdmax(p)-grdmin(p)))/100;
   x(2,i)=xin(2,1)+cx2*xin(2,1)*(grdmin(p)+rand(1)*(grdmax(p)-grdmin(p)))/100;
   x(3,i)=xin(3,1)+cx3*xin(3,1)*(grdmin(p)+rand(1)*(grdmax(p)-grdmin(p)))/100;
end
for
i=((floor((ind(1,p)+ind(2,p)+ind(3,p))/2))+1):(floor((ind(1,p)+ind(2,p)+ind(3,p)+ind(4,p
))/2)); %i=curious individuals
   x(1,i)=xin(1,1)+cx1*xin(1,1)*(crsmin(p)+rand(1)*(crsmax(p)-crsmin(p)))/100;
   x(2,i)=xin(2,1)+cx2*xin(2,1)*(crsmin(p)+rand(1)*(crsmax(p)-crsmin(p)))/100;
   x(3,i)=xin(3,1)+cx3*xin(3,1)*(crsmin(p)+rand(1)*(crsmax(p)-crsmin(p)))/100;
end
for
i=((floor((ind(1,p)+ind(2,p)+ind(3,p)+ind(4,p))/2))+1):(floor((ind(1,p)+ind(2,p)+ind(3,p
)+ind(4,p)+ind(5,p))/2)); %i=normal individuals
   x(1,i)=xin(1,1)+cx1*xin(1,1)*(normin(p)+rand(1)*(normax(p)-normin(p)))/100;
   x(2,i)=xin(2,1)+cx2*xin(2,1)*(normin(p)+rand(1)*(normax(p)-normin(p)))/100;
   x(3,i)=xin(3,1)+cx3*xin(3,1)*(normin(p)+rand(1)*(normax(p)-normin(p)))/100;
end
```

```
for
i=((floor((ind(1,p)+ind(2,p)+ind(3,p)+ind(4,p)+ind(5,p))/2))+1):(floor((ind(1,p)+ind(2,p
)+ind(3,p)+ind(4,p)+ind(5,p)+ind(6,p))/2)); %i=conservative individuals
   x(1,i)=xin(1,1)+cx1*xin(1,1)*rand(1)*conmax(p)/100;
   x(2,i)=xin(2,1)+cx2*xin(2,1)*rand(1)*conmax(p)/100;
   x(3,i)=xin(3,1)+cx3*xin(3,1)*rand(1)*conmax(p)/100;
end
a=0;
for i=1:(floor((ind(1,p)+ind(2,p)+ind(3,p)+ind(4,p)+ind(5,p)+ind(6,p))/2));
   y(i)=9*x(1,i)^2+9*x(2,i)^2+9*x(3,i)^2-1359.42*x(1,i)+182.88*x(2,i)-279011.2909;
   if y(i)<ymax;
      ymax=y(i);
      xin(1,1)=x(1,i);
      xin(2,1)=x(2,i);
      xin(3,1)=x(3,i);
      a=i; %fittest individuals, a=i'th individual
   end
end

if a==0;
   bolum1=1;bolum2=0;
   x1arti=0;
   x1eksi=0;
   x2arti=0;
   x2eksi=0;
   x3arti=0;
   x3eksi=0;
end
end %bolum2 end
w=p;
if p~=3; %aging
   if a>ind(1,p)+ind(2,p)+ind(3,p); %checking fittest
      if a>ind(1,p)+ind(2,p)+ind(3,p)+ind(4,p)+ind(5,p);
         s=s+1;
```

```
            if s==10;p=3;
            end
        elseif p~=2;
            f=f+1;
            if f==20;p=2;
            end
        end
    end
end
if a~=0; %credit assignRENEWAL
    if a>ind(1,w);
        if a>ind(1,w)+ind(2,w);
            if a>ind(1,w)+ind(2,w)+ind(3,w);
                if a>ind(1,w)+ind(2,w)+ind(3,w)+ind(4,w);
                    if a>ind(1,w)+ind(2,w)+ind(3,w)+ind(4,w)+ind(5,w);
                        kazanan=6;
                    else kazanan=5;
                    end
                else kazanan=4;
                end
            else kazanan=3;
            end
        else kazanan=2;
        end
    else kazanan=1;
    end
    j=kazanan;ind(j,w)=ind(j,w)+1;
    if ind(j,w)>indmax;
        ind(j,w)=indmax;
    end
end
if w~=1; %killing the unused
    if w==2;
        g=randperm(3);
```

```
        j=g(1,1);
        ind(j,w)=ind(j,w)-1;
        if ind(j,w)<indmin;
           ind(j,w)=indmin;
        end
    else g=randperm(5);
        j=g(1,1);
        ind(j,w)=ind(j,w)-1;
        if ind(j,w)<indmin;
           ind(j,w)=indmin;
        end
    end
end

end %iteration end
if  p==1;
    devam=1;
else devam=0;
end
end %while end
xin(1,1)
xin(2,1)
xin(3,1)
end %end of loop
toc
```